

**INTEGRATION OF THERMAL INSULATION MATERIAL AND
ACTIVE MOVING AIR CAVITY VENTILATION IN A COOL ROOF
SYSTEM FOR ATTIC TEMPERATURE REDUCTION**

TAN KAI FENG


**A project report submitted in partial fulfilment of the
requirements for the award of Bachelor of Engineering
(Honours) Mechanical Engineering**

**Lee Kong Chian Faculty of Engineering and Science
Universiti Tunku Abdul Rahman**

April 2022

DECLARATION

I hereby declare that this project report is based on my original work except for citations and quotations which have been duly acknowledged. I also declare that it has not been previously and concurrently submitted for any other degree or award at UTAR or other institutions.

Signature : 

Name : Tan Kai Feng

ID No. : 1702987

Date : 4/6/2022

APPROVAL FOR SUBMISSION

I certify that this project report entitled **“INTEGRATION OF THERMAL INSULATION MATERIAL AND ACTIVE MOVING AIR CAVITY VENTILATION IN A COOL ROOF SYSTEM FOR ATTIC TEMPERATURE REDUCTION”** was prepared by **TAN KAI FENG** has met the required standard for submission in partial fulfilment of the requirements for the award of Bachelor of Engineering (Honours) Mechanical Engineering at Universiti Tunku Abdul Rahman.

Approved by,

Signature

:



Supervisor

:

Ir. Ts. Dr. Yew Ming Chian

Date

:

April 2022

Signature

:

-

Co-Supervisor

:

-

Date

:

-

The copyright of this report belongs to the author under the terms of the copyright Act 1987 as qualified by Intellectual Property Policy of Universiti Tunku Abdul Rahman. Due acknowledgement shall always be made of the use of any material contained in, or derived from, this report.

© 2022, Tan Kai Feng. All right reserved.

ACKNOWLEDGEMENTS

I would like to thank everyone who contributed to the successful completion of this project. I would like to express my gratitude to my research supervisor, Dr Yew Ming Chian for his invaluable advice, guidance and his enormous patience throughout the development of the research.

In addition, I would like to show my sincere appreciation to the mechanical workshop staff, Mr Ho Chan Cheong, Encik Muhammad Izhar Bin Mohamad Pauzi, and Encik Mohd Hanis Bin Nazli for providing assistance and guidance on the operation of workshop equipment and machines during the fabrication of the prototype.

Lastly, I would also like to express my gratitude to my loving parents and friends who helped and encouraged me when I was downhearted.

ABSTRACT

The roof is the primary heat source for landed buildings since it is exposed to the sun. This will lead to significant heat gain in the attic, causing thermal discomfort for the indoor dwellers and increasing cooling loads. A cool roof system can provide thermal insulation to the attic, preventing excessive heat gain and lowering the cooling load, saving electricity consumption from air conditioning systems. Thus, cool roofs' attic temperature reduction performance with passive thermal insulation and active ventilation components, including vegetation layer, lightweight foam concrete (LFC) roof slab of density 1250 kg/m^3 , and active moving air cavity (MAC) with solar-powered fans (S-P Fs) are studied. Five roof models were built applying these elements in stages, with the first model as a reinforced concrete roof to be the base model. All roof models were inclined at 30° . The experiment was conducted indoors by projecting two 500 W halogen spotlights right angle at each roof model, and the temperature at the ambient, roof surface, attic, and MAC was measured with k-type thermocouples for 30 minutes, and the variation was shown in a plot of temperature versus times for each roof model. The temperature cooling performance of each model was compared against the predecessor design and base model. A significant drop in attic temperature increment was observed when the MAC was installed under the LFC roof slab, with a maximum attic temperature of $28.9 \text{ }^\circ\text{C}$ and an average increment rate of $0.05 \text{ }^\circ\text{C}/\text{min}$, 50% slower than the previous roof model. When the vegetation layer and S-P Fs were added, the temperature in the attic was almost maintained at a constant level of $26.9 \text{ }^\circ\text{C}$ with a rate of $0.003 \text{ }^\circ\text{C}/\text{min}$, which is a staggering 96.77% lower than the based model. In brief, this experiment outcome showed the effectiveness of the cool roof system integrating a vegetation layer, LFC, and an active MAC in keeping the attic cool.

TABLE OF CONTENTS

DECLARATION		i
APPROVAL FOR SUBMISSION		ii
ACKNOWLEDGEMENTS		iv
ABSTRACT		v
TABLE OF CONTENTS		vi
LIST OF TABLES		ix
LIST OF FIGURES		x
LIST OF SYMBOLS / ABBREVIATIONS		xii
LIST OF APPENDICES		xiii
CHAPTER		
1	INTRODUCTION	1
1.1	General Introduction	1
1.2	Importance of the Study	3
1.3	Problem Statement	4
1.4	Aim and Objectives	5
1.5	Scope and Limitation of the Study	5
1.6	Contribution of the Study	6
1.7	Outline of the Report	6
2	LITERATURE REVIEW	7
2.1	Malaysia Electrical Energy Usage	7
2.2	Heat Transfer in Cool Roof Design	8
2.3	Contemporary Cool Roof Design	10
2.3.1	Extensive Green Roof System	11
2.3.2	Lightweight Foam Concrete (LFC) Roof Tile	16
2.3.3	Active Moving Air Cavity (MAC)	19
3	METHODOLOGY AND WORK PLAN	22
3.1	Introduction	22

3.2	Roof Model Designs	25
3.2.1	Roof Model I (Reinforced Concrete Roof Slab)	26
3.2.2	Roof Model II (LFC Roof Slab)	26
3.2.3	Roof Model III (LFC Roof Slab with MAC)	27
3.2.4	Roof Model IV (LFC Roof Slab with Active MAC Fitted with S-P Fs)	27
3.2.5	Roof Model V (LFC Roof Slab Topped with Vegetation Layer with Active MAC Fitted with S-P Fs)	27
3.3	Roof Model Components	28
3.3.1	Vegetation Layer	28
3.3.2	Lightweight Foam Concrete (LFC) Roof Slab	30
3.3.3	Moving Air Cavity (MAC)	31
3.3.4	Solar-Powered Fans (S-P Fs)	32
3.4	Experiment Set-up	33
4	RESULTS AND DISCUSSION	34
4.1	Roof Model I (Reinforced Concrete Roof Slab)	34
4.2	Roof Model II (LFC Roof Slab)	35
4.3	Roof Model III (LFC Roof Slab with MAC)	36
4.4	Roof Model IV (LFC Roof Slab with Active MAC Fitted with S-P Fs)	38
4.5	Roof Model V (LFC Roof Slab Topped with Vegetation Layer with Active MAC Fitted with S-P Fs)	39
4.6	Comparison between different roof models	41
4.6.1	Variation in Roof Surface Temperature	41
4.6.2	Variation in Attic Temperature	43
4.6.3	Variation in MAC Temperature	45
4.7	Summary	47
5	CONCLUSIONS AND RECOMMENDATIONS	49
5.1	Conclusions	49

5.2	Recommendations for Future Work	50
	REFERENCES	52
	APPENDICES	60

LIST OF TABLES

Table 2.1: Green Roof in Malaysia (Chow and Bakar, 2016).	14
Table 2.2: Comparison of The RTTV Value for Reinforce Concrete Roof and Green Roof (Pandey, Hindoliya and Mod, 2013).	16
Table 2.3: The Average Increment Rate of Attic Temperature for Various Roof Tiles (Yew et al., 2021).	18
Table 3.1: Components for Each Roof Model.	22
Table 4.1: Results Summary.	48

LIST OF FIGURES

Figure 1.1: Cool Roof System (BMI, 2021).	2
Figure 2.1: Final Energy Consumption by Sector (Suruhanjaya Tenaga, 2019).	7
Figure 2.2: Heat Transfer Mechanism of Cool Roof Design (Yew et al., 2013).	9
Figure 2.3: Pitched Green Roof (ZinCo, n.d.).	11
Figure 2.4: Components of Extensive Green Roof System (Siew, Chin and Sakundarini, 2019).	12
Figure 2.5: Experimental Model of Green Roof (Pandey, Hindoliya and Mod, 2013).	15
Figure 2.6: Comparison Between the Performance of (a) Metal Roof and (b) LFC Roof (Yew et al., 2021).	18
Figure 2.7: Heat Removed from a Cavity with Various Roof Steepness (Lee et al., 2009).	20
Figure 3.1: The Experiment Process Flow Chart.	24
Figure 3.2: Roof Models I, II, III, IV and V.	26
Figure 3.3: The Dimension of Attic in Millimeters.	28
Figure 3.4: Wood Tray.	29
Figure 3.5: The Schematic Diagram of The Vegetation Layer.	29
Figure 3.6: Dimension of MAC in Millimeters.	31
Figure 3.7: Aluminium Sheet (Left) and Aluminium Foil (Right).	32
Figure 3.8: Wire Mesh.	32
Figure 3.9: Set Up of Roof Model.	33
Figure 4.1: Graph of Temperature (°C) Versus Time (min) for Roof Model I (Reinforce Concrete Roof Slab).	34
Figure 4.2: Graph of Temperature (°C) Versus Time (min) for Roof Model II (LFC Roof Slab).	35

Figure 4.3: Graph of Temperature ($^{\circ}\text{C}$) Versus Time (min) for Roof Model III (LFC Roof Slab with MAC).	36
Figure 4.4: Graph of Temperature ($^{\circ}\text{C}$) Versus Time (min) for Roof Model IV (LFC Roof Slab with Active MAC Fitted with S-P Fs).	38
Figure 4.5: Graph of Temperature ($^{\circ}\text{C}$) Versus Time (min) for Roof Model V (LFC Roof Slab Topped with Vegetation Layer with Active MAC Fitted with S-P Fs).	39
Figure 4.6: Variation in Roof Surface Temperature ($^{\circ}\text{C}$) for Different Models.	42
Figure 4.7: Variation in Attic Temperature ($^{\circ}\text{C}$) for Different Models.	43
Figure 4.8: Temperature Increment (%) on Roof Surface and Attic and Average Attic Temperature Increment Rate ($^{\circ}\text{C}/\text{min}$).	44
Figure 4.9: Variation in MAC Temperature ($^{\circ}\text{C}$) for Different Models.	46

LIST OF SYMBOLS / ABBREVIATIONS

c_p	specific heat capacity, J/(kg·K)
h	height, m
K_d	discharge coefficient
M	mass flow rate, kg/s
P	pressure, kPa
P_b	back pressure, kPa
R	mass flow rate ratio
T	temperature, K
v	specific volume, m ³
α	homogeneous void fraction
η	pressure ratio
ρ	density, kg/m ³
ω	compressible flow parameter
ID	inner diameter, m
MAP	maximum allowable pressure, kPa
MAWP	maximum allowable working pressure, kPa
OD	outer diameter, m
RV	relief valve

LIST OF APPENDICES

Appendix A: Figures	60
Appendix B: Tables	64

CHAPTER 1

INTRODUCTION

1.1 General Introduction

Malaysia is located in a tropical region with a hot and humid climate all year round, so air conditioning is necessary for home dwellers or building occupants to maximise necessary for home dwellers or building occupants to maximise indoor thermal comfort. Furthermore, people tend to improve their lifestyle in many ways by installing air conditioners for cooling the building space in hot weather is indispensable. However, the air conditioning system, also known as HVAC or ACMV system, is the most energy-consuming equipment in a building. Indeed, the air conditioning system contributes to 20% of the building sector's overall electricity usage worldwide (Hu, Yan and Qian, 2019). In the case of Malaysia, about 50% of the energy consumption in an ordinary building attributes to the HVAC system (Tang and Chin, 2017a).

The high energy consumption of the air-conditioning system may be attributed to the poor thermal insulation of the building (Ramlee, Naveen and Jawaid, 2021). The general application of air conditioning across every household has elevated electrical energy consumption. Thus, passive building thermal insulation that reduces the cooling load is required to alleviate the energy demand. For instance, the design of green envelop incorporated into the building has effectively achieved energy savings, especially in the hot climate experienced by Malaysia, as proven by various authors (Azis, 2021; Abd Rahman, Lim and Fazlizan, 2021). The green envelope can be designed on the wall and roof of the building.

Residential and commercial buildings are claimed to have high energy saving potential; with the integration of green insulation components, a reduction of cooling load as high as 25% is able to achieve by residential buildings (Azis, 2021). In other words, the passive cool building design with effectual thermal insulation can provide comfortable indoor temperature for the occupants and thus reduce the usage of active air conditioning, hence minimising the electrical utility (Ng et al., 2019). This is because the insulating material applied on the wall and roof can reduce the thermal conductivity,

resulting in lower heat gain in the building. Besides using traditional thermal insulation material, vegetated envelop also yields a promising energy-saving outcome in tropical climates (Azis, 2021).

The main source of heat transferring into the building is from the sun. The area of a building that exposes the most and the longest to the sun is the roof. The incident solar radiation on the roof can reach 297 W/m^2 average peak direct radiation at noon and the absolute peak direct radiation can reach a staggering value of 865 W/m^2 at 2 pm (Ministry of Economic Affairs, 2018). The solar radiation reaching the roof will increase the roof's surface temperature, and the heat will eventually transfer into the attic via conduction through the roof layer. The attic is the space between the roof and ceiling. The heat gain in the attic will then transfer into the occupant space below the ceiling, increasing the cooling load and compromising thermal comfort. Thus, an intensive energy-consuming air conditioning system is needed to cool down the space. In order to cut down electricity consumption of the air conditioning, the cooling load and heat gain must be reduced, and a cool roof is a prominent solution to that as it insulates the attic from the thermal transfer from the solar radiation.

A simple cool roof system consists of a reflective roof that aims to reflect the solar radiation and thermal insulation layer, such as roof solar collectors or moving air cavity (MAC) that ventilates the heat, as illustrated in Figure 1.1. The goal of these components is to provide passive cooling effects to the attic space.

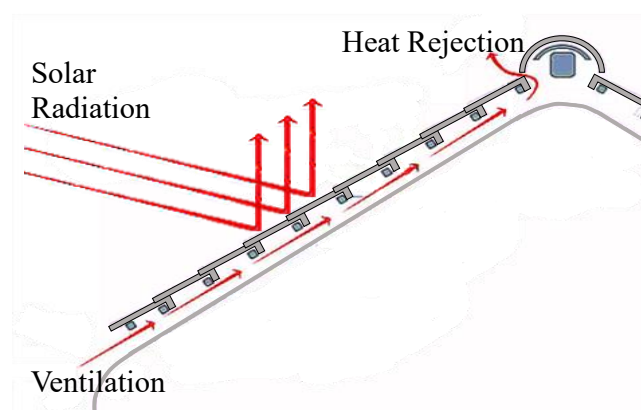


Figure 1.1: Cool Roof System (BMI, 2021).

It can also integrate other thermal insulation materials such as rock wool, gypsum board, foam concrete, and even a green vegetated layer. The green vegetated layer can also provide thermal insulation and prevent heat flux from being transferred into the attic (Bevilacqua, 2021). The active cooling effect can also be attained by installing solar-powered fans (S-P Fs) at the MAC inlet to achieve a higher heat rejection rate through an increased airflow rate. The fan is entirely powered by solar energy, so it is sustainable yet economical.

This project will study the effectiveness of a cool roof integrating passive thermal insulation and active ventilation components, which comprise a vegetation layer, lightweight foam concrete (LFC) roof slab, and an active MAC retrofitted with S-P Fs.

1.2 Importance of the Study

This study is focusing on the attic temperature reduction performance of the cool roof design integrating passive and active components. The passive components include the vegetation layer on top of an LFC roof slab. This combination resembles an extensive green roof. The active components will employ S-P Fs to actively ventilate the MAC for forced convection heat rejection. The reduction in attic temperature will eventually reduce the cooling load in the living space, hence minimizing the energy consumption of the air conditioning system while ensuring the occupants' thermal comfort.

Therefore, the experimental findings of this study may provide insight into the thermal insulation performance of the proposed cool roof system. This study can also motivate implementing an advanced cool roof system integrating modern thermal insulation technologies such as green roofs, LFC roof slabs, and moving air cavities in future building developments. Furthermore, this study can serve as an inspiration to help develop, commercialize and industrialize cool roof systems for commercial and residential buildings in Malaysia as well as encourage the utilisation of green roof systems in green building design by providing concrete experimental data regarding the cooling effects that demonstrate the potential of the cool roof system.

1.3 Problem Statement

Nowadays, the world energy supply relies heavily on burning fossil fuels that cause adverse effects such as global warming and climate change (U.S. Department of Energy, 2016). For instance, 95% of the electricity supply in Malaysia is generated from non-environmentally friendly and non-renewable fossil fuels (Suruhanjaya Tenaga, 2017a). The building sector is one of the main drivers of high energy consumption. In Malaysia, about 39% of the total energy demand was induced by building sectors (Shaikh et al., 2017). Among the building sectors, the electrical energy usage is 46%, 32% and 21%, respectively for the industrial, commercial and residential sectors (Azis, 2021).

Aqilah et al. (2021) stated that the residential sector's electrical power has shown an increasing trend globally. This may be attributed to the expanding world's population has increased the energy demand in every household. Meanwhile, in Malaysia, the residential sector showed an average annual energy growth rate of 12% from 1995 to 2015, the highest among the building sectors (Suruhanjaya Tenaga, 2017a).

The air conditioning system consumes most of the energy demand in a building. This is because the extreme ambient temperature of Malaysia increases the temperature in the attic and subsequently the indoor space, jeopardizing the thermal comfort of the building occupants. Hence, they intensively use air conditioning to achieve a cooler indoor environment.

Therefore, the problem definition of this study is how to reduce the attic temperature so that more electrical energy can be saved from the air conditioning system for a sustainable built environment. To tackle this issue, conventional roof designs in Malaysia such as metal deck roofs or reinforced concrete roofs, which are thermally conductive materials, can be improved to reduce the heat transfer into the attic so that the indoor cooling load will decrease and save electricity.

Henceforth, a cool roof system that lowers the attic temperature passively and actively is designed with thermal insulation materials that integrate a vegetation layer and LFC roof tile with the addition of active MAC fitted with S-P Fs. The attic temperature can be successfully reduced with the passive and active cooling strategies introduced in the cool roof design.

1.4 Aim and Objectives

This project aims to design a cool roof system that can reduce the attic temperature. In order to achieve the aim, the following objectives are formulated:

- a) To design and develop small scale cool roof models.
- b) To evaluate the performance of thermal insulation materials with the integration of vegetation layer and LFC roof tile.
- c) To determine the combination of thermal insulation materials and MAC-solar powered fans for attic temperature reduction.

1.5 Scope and Limitation of the Study

The scope of this study is to investigate the thermal insulation and heat rejection performance of a small scale cool roof system implementing both passive and active methods. The passive system of the cool roof model utilizes thermal insulation components, a vegetation layer planted with ferns and wormwood and a lightweight form concrete roof slab. The passive system will also include a MAC that rejects the heat from the atmosphere with natural ventilation. The vegetation layer will be integrated with the lightweight form concrete roof slab to imitate an extensive green roof system. In addition, the active system of the cool roof model will be built by retrofitting seven S-P Fs at the inlet of the MAC to induce forced convection to enhance the heat rejection rate with a greater airflow rate. The components are integrated into the roof model one at a time, and five roof models are proposed and their attic temperature reduction performance will be compared amongst each other. In addition, this study focused on low rise buildings instead of high rise because the heat transferred from the roof into the building accounted for major indoor temperature rise for low rise buildings.

Nonetheless, the scope of study inadvertently imposed some limitations. The limitations are:

- Due to the limited budget for the project, the cool roof models have to be scaled down.
- The cool roof models will be built on an attic made of acrylic with a base area of 355 mm × 340 mm, which is a scaled-down model. Thus, the performance in reducing attic temperature may deviate from the actual scale cool roof installed on a building. However, this study only focused

on showing the improvement of the roof models in reducing attic temperature compared to the base model and previous model.

- The extensive green roof model will exclude some layers to simplify the model, so the thermal conductivity of the excluded layers is omitted in the study.
- The study is only limited to tropical climates; the design of the cool roof system may not be applicable to temperate climates and the results from the study may not reflect the performance of the cool roofs in those countries with four seasons.

1.6 Contribution of the Study

This study contributes to the encouragement of applying cool roof systems, which helps to reduce attic temperature and eventually lower cooling loads to save electricity consumption from air conditioning systems. This is done by proving the effectiveness of the cool roof system in keeping the attic cool, which incorporated several passive thermal insulations: vegetation layer, LFC roof slab, MAC, and an active cooling element which is S-P Fs. This also promotes the application of green roof systems as represented by the vegetation layer in the study. Additionally, it also promotes the use of renewable solar energy with the solar panel when the S-P Fs are applied for active ventilation in the MAC.

1.7 Outline of the Report

In Chapter 2, the report first reviewed Malaysia's electrical energy usage in the building industry, especially in the air conditioning system. The literature review also included the heat transfer mechanism in a cool roof system and several cool roof designs in the present day.

Next, Chapter 3 described five roof model designs for the study along with the method to construct each roof component. It also described the methodology and set-up of the experiment.

Then, Chapter 4 discussed the result showing the trend of the temperature increment against times of different parts of each roof model and compared their cooling performance with the predecessor design and base model. The report ended with a concluding statement and recommendations for future studies in Chapter 5.

CHAPTER 2

LITERATURE REVIEW

2.1 Malaysia Electrical Energy Usage

Malaysia is located near the equator, which gives it a hot and humid climate throughout the year. The dry bulb temperature of Malaysia averages at 26.9 °C all year long, with an average peak temperature of 32 °C in the afternoon, whereas the humidity ratio averages at 18.3 g/kg throughout the day (Tang and Chin, 2017). However, this temperature and humidity are not able to attain the recommended thermal comfort for the buildings or house occupants. According to the Malaysia Standard 1525 (2014), the recommended dry bulb temperature and relative humidity for an air-conditioned space for managing the thermal comforts of building occupants are between 24 °C and 26 °C and between 50% and 70%, respectively. Thus, Malaysians will install air conditioners to cool down their home and achieve a comfortable temperature, which is very energy-consuming.

Suruhanjaya Tenaga (2019) provided the statistic for the energy consumption for different sectors, as shown in Figure 2.1.

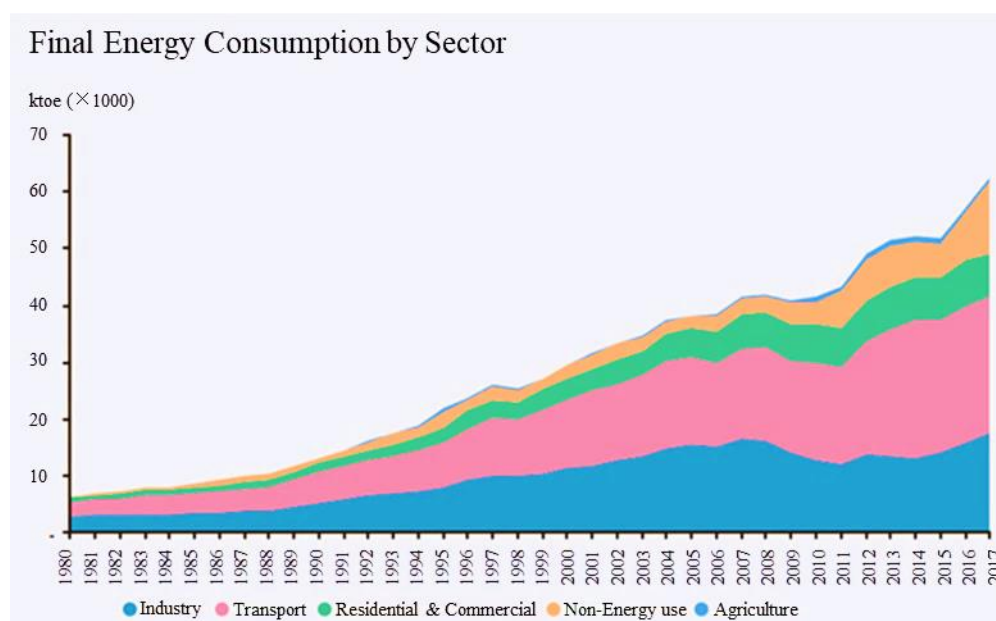


Figure 2.1: Final Energy Consumption by Sector (Suruhanjaya Tenaga, 2019).

It shows that the energy consumption for every sector has increased rapidly since 1980. For the residential and commercial sectors, the energy consumption has increased from 826 ktoe in 1980 to 7796 ktoe in 2017 (Suruhanjaya Tenaga, 2019).

According to the Suruhanjaya Tenaga (2017b), about 20.7% of the national energy consumption has been from the residential sector in the past few years. Moreover, it is expected that Malaysian household energy consumption will escalate further due to more electrical appliances, better financial status, and new norms in lifestyle (Ministry of Energy, 2017). In fact, due to the hot climate in Malaysia, it is widespread for Malaysians to have installed at least one air conditioning unit in their house.

It is reported that the air conditioner consumes the most electrical energy in a house, contributing 28% to 46% of the total electrical energy consumption (Ranjbar et al., 2017). A survey done by Hisham et al. (2019) also figured a similar degree of electricity consumption by air conditioning units, between 30% and 50% of the total electricity consumption.

The majority favour colder room environments than the recommended design temperature given by MS 1525, which will cost more electricity. Most home dwellers prefer to set the air conditioner temperature between 19 °C and 25 °C, colder than the standard recommended value (Sena et al., 2021). This is also supported by a survey conducted by Hisham et al. (2019) that states 92% of the sample dwellers would set the air conditioner temperature below 24 °C.

Increasing energy consumption is expected in the residential sector in the near future, so it has the potential in helping to diminish the overall electrical energy usage (Ahmed et al., 2017). Therefore, in order to reduce electricity consumption, strategies for saving electricity have to be executed in residential buildings (Sena et al., 2021). On top of that, integrating cool roofs in residential houses is one of the solutions as it can reduce heat load in the homes and hence decline energy consumed by the air conditioning system.

2.2 Heat Transfer in Cool Roof Design

A typical passive cool roof design consists of thermal insulation integrated on top of the roof and a MAC, also known as a solar roof collector, installed below the roof deck. As for an active cool roof, fans may be fitted at the inlet of the

MAC to increase the air velocity and hence expel the heat more effectively. Figure 2.2 shows the schematic diagram and the heat transfer mechanism of a typical cool roof design with a reflective coating applied on top of the roof deck and an active MAC with fans installed at the inlet of the cavity (Yew et al., 2013).

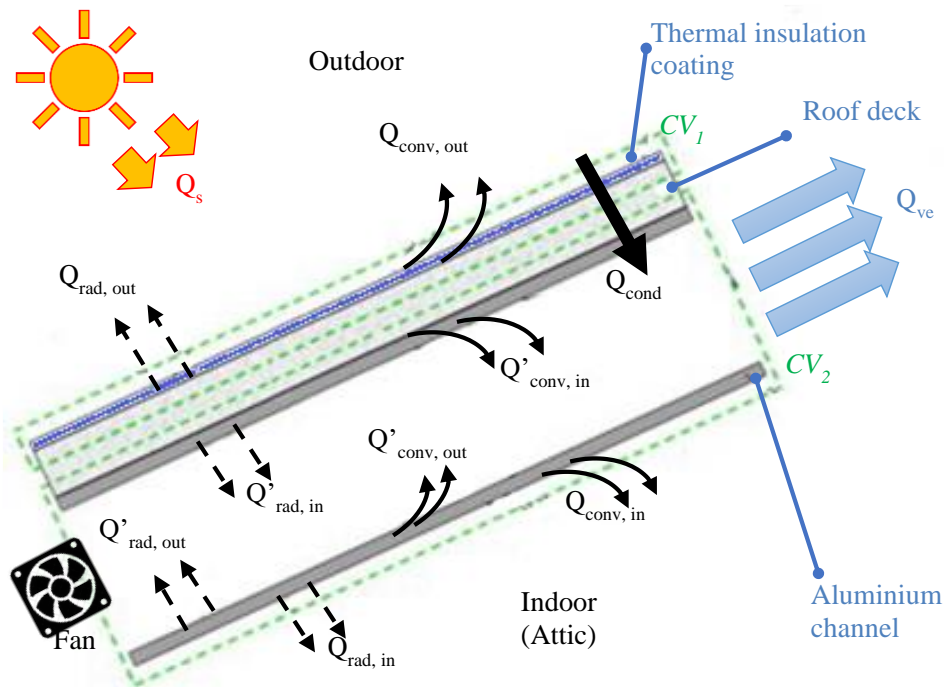


Figure 2.2: Heat Transfer Mechanism of Cool Roof Design (Yew et al., 2013).

Based on the second law of thermodynamics, heat can only flow from a hot environment to a cold environment. In other words, it cannot flow in the opposite direction from cold to hot environment. Since the ambient temperature outside the attic is generally higher than the temperature inside the attic, heat will flow in a single direction from outside, passing through the cool roof and eventually into the attic space.

According to Yew et al. (2018), the heat transfer mechanism of a cool roof can be separated into two control volumes which are control volume one (CV_1): heat transfer from the ambient atmosphere to the thermal insulation layer, and control volume two (CV_2): heat transfer from the roof deck to the MAC and attic at last. As shown below, equation (2.1) is written to represent the control volume one (CV_1).

$$Q_s = Q_{rad,out} + Q_{conv,out} + Q_{cond} \quad (2.1)$$

where

- Q_s = Heat energy gained from the solar radiation, W
- $Q_{rad,out}$ = Radiation heat reflected away from the insulation coating, W
- $Q_{conv,out}$ = Convection heat transfer from the roof deck, W
- Q_{cond} = Conduction heat transmitting through the roof deck, W

Besides, equation (2.2) represents the control volume two (CV_2).

$$Q_{cond} = Q_{rad,in} + Q_{conv,in} + Q_{ve} \quad (2.2)$$

where

- Q_{cond} = Heat conduction through the roof deck, W
- $Q_{rad,in}$ = Heat transfer into the attic through radiation, W
- $Q_{conv,in}$ = Heat transfer into the attic through convection, W
- Q_{ve} = Amount of heat ventilated out from the MAC into the atmosphere, W

Equation (2.3) shows the formula for computing the amount of heat being ventilated out from the MAC.

$$Q_{ve} = \dot{m}C_p(T_{out} - T_{in}) \quad (2.3)$$

where

- Q_{ve} = Heat exhaust out from the MAC into the atmosphere, W
- \dot{m} = Mass flow rate of the moving air, kg/s
- C_p = Specific heat at 1 atm, J/kg K
- T_{out} = Outlet air temperature of the MAC, K
- T_{in} = Inlet air temperature of the MAC, K

2.3 Contemporary Cool Roof Design

A conventional roof design can be made of metal, clay, or concrete roof tile, with insulation directly above the ceiling. However, modern roof design has a sophisticated yet simple mechanism to help provide more thermal insulation and

cooling effect to the attic space, hence called the cool roof. A simple cool roof design can incorporate a highly reflective tile surface, insulations below the roof and channels that promote natural airflow for heat removal. Different cool roof features such as green or vegetated roofs, LFC tile, and active MAC are reviewed.

2.3.1 Extensive Green Roof System

Green roofs or vegetated roofs have been pervasively applied in European countries. A green roof is able to provide some cooling effect to the building, thereby declining the energy consumption for the air conditioning system (Chow and Bakar, 2016). This is because the substrate layer and the foliage height act as an excellent thermal resistant barrier that prevents solar radiation energy from transferring into the building interior. Additionally, the green roof can also alleviate the negative effect of heat islands from metal or concrete roof tile, which will also help reduce air conditioning energy usage (Hui and Chan, 2008). Figure 2.3 shows a vegetated roof with a slope in a temperate climate country.



Figure 2.3: Pitched Green Roof (ZinCo, n.d.).

To design a green roof system, several green roof design guidelines were reviewed. Unfortunately, there is no available guideline published in Malaysia yet, so guidelines from other countries with well developed green roof

systems are reviewed, such as the Forschungsgesellschaft Landschaftsentwicklung Landschaftsbau, FLL 2008 Green Roofing Guidelines from Germany, the Technical Guidelines for Green Roof Systems in Hong Kong, and the Singapore CUGE Standards. However, the German FLL is not suitable to be referred to in Malaysia due to differences in climate conditions between both countries as Malaysia has a tropical climate whereas Germany has a temperate climate (Siew, Chin and Sakundarini, 2019). In Malaysia, only a few studies have been conducted on the recommendation of design for the green roof system.

An extensive green roof consists of different layers where different guidelines propose a slightly different arrangement of the layer components, but the components are generally the same. Figure 2.4 shows that a green roof is made of different components arranged in layer form.

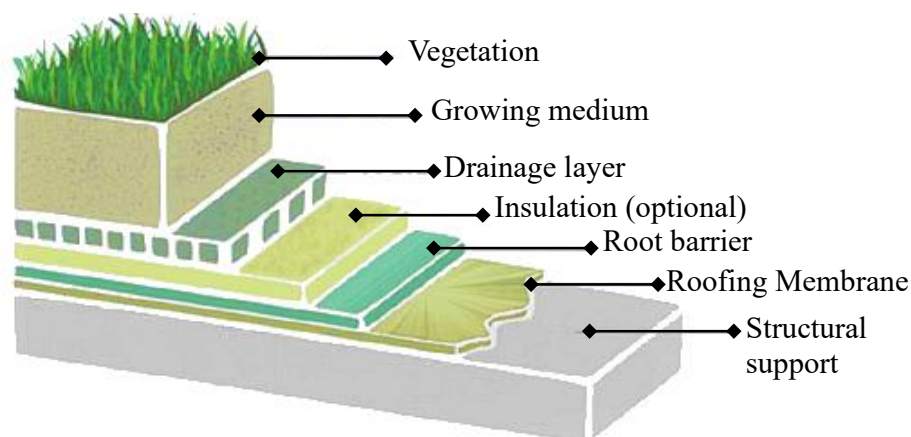


Figure 2.4: Components of Extensive Green Roof System (Siew, Chin and Sakundarini, 2019).

Extensive green roofs have a substrate thickness layer of less than 200 mm and require less maintenance than intensive green roofs since the choice of plants selected generally need minimal attention and care but can survive well (Siew, Chin and Sakundarini, 2019). This claim is also supported by the Technical Guidelines for Green Roof Systems in Hong Kong that drought-resistant plant species or CAM (Crassulacean Acid Metabolism) plants are suitable and well adapt for rooftop environments without the presence of irrigation since yearly rainfall is enough to hydrate the vegetation (Hui, 2011). Besides that, extensive

green roofs are also characterised by low cost, do not require an irrigation system, and have a low saturated weight of 60 kg/m² to 150 kg/m² (Hui, 2011).

Furthermore, on the selection of plants, all the guidelines unanimously agree that Sedum (a type of CAM plant) is the primary choice for extensive green roofs because of its adaptability and survivability to extreme heat from solar radiation, scarce nutrients, strong wind, and limited growing space for the roots (FFL, 2002; Tan and Sia, 2008; Hui, 2011). Besides, sedum is also highly recommended for pitched roofs because it can avoid erosion and retain a large amount of water. However, Sedum is an exotic plant species that are not suitable to be grown in Malaysia's hot and humid climate. Therefore, a study was done by Krishman, Ahmad and Mohamad (2013) to identify the suitable native plant species for Malaysia green roofs. It was later found that ferns are also ideal as green roof plant as it poses characteristics similar to Sedum, which are fast-growing, dense roots and high penetration that promotes binding to the substrate, and succulent leaves. The further investigation reviewed that fern are also a member of CAM plants.

The green roof systems have been trending the many countries such as Singapore, Hong Kong, and predominantly European countries. Nonetheless, green roofs are still not widely adopted in Malaysia yet. According to Chow and Bakar (2016), only a few buildings in Malaysia have incorporated green vegetated roofs to promote green and sustainable development for the past 15 years. Table 2.1 shows the buildings that have green roof designs chronologically.

Table 2.1: Green Roof in Malaysia (Chow and Bakar, 2016).

Building	Green roof type	Completion year
Rice garden museum (Laman Padi), Langkawi	Intensive	1998
Ministry of Finance, Putrajaya	Extensive and Intensive	2002
Putrajaya International Convention Centre (PICC), Putrajaya	Extensive and Intensive	2003
Putrajaya City Hall, Putrajaya	Extensive	2004
Malaysian Design Technology Centre (MDTC), Cyberjaya	Extensive	2004
Serdang Hospital	Intensive	2005
Faculty of Social Sciences and Humanities, Universiti Kebangsaan Malaysia	Extensive	2007
Sime Darby Oasis, Damansara	Extensive	2009
KL Sentral Park	Intensive	2009
Newcastle University Medicine Malaysia, Nusajaya	Extensive	2011
Laman PKNS, Shah Alam	Intensive	2013
Heriot-Watt University, Putrajaya	Extensive	2014
Tun Razak Exchange (TRX)	Intensive	2016

The number of buildings with green roofs is notably low despite the benefits of reducing heat island, reducing heat flux to the building interior, reducing electricity consumption, increasing greenery in the city and so on, due to the challenges confronted by the developers. Ismail et al. (2012) have surveyed the contributing factors that impede the development of green roofs in Malaysia and identified that the factors comprise former failure, expensive cost, complex maintenance, lack of professionals and scientific study, the anxiety of unforeseen risk, no standard and guideline for the design, and speculate that green roofs are fire hazards. Other than that, building operators in Malaysia do not have much experience in managing and maintaining green roofs, which

leads to poor maintenance (Chow and Bakar, 2016). Lack of suppliers of green roofs, expensive installation costs, and materials also dissuade local developers from implementing green roofs. Lastly, there is no standard or guideline on green roof system design being published in Malaysia (Ismail, Samad and Rahman, 2008). Thus, the developers and contractors do not have any guidance in designing and installing green roofs in a certified way.

In order to overcome the aforementioned challenges and promote the adoption of green roofs in future buildings, the Malaysian government has first to provide a complete and comprehensive guideline and even initiate incentives for developers that have green roofs as part of their building projects.

Pandey, Hindoliya and ModPandey conducted an experiment, (2013) and the effectiveness of green roofs in reducing attic temperature is proven. Figure 2.5 shows the green roof model of the investigation, which is made of a reinforced concrete roof slab of 100 mm thickness, 300 mm layer of substrate and a layer of shrubs installed on a 1×1×1 m brick room.

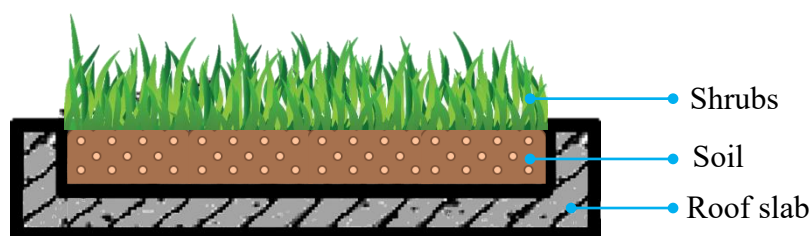


Figure 2.5: Experimental Model of Green Roof (Pandey, Hindoliya and Mod, 2013).

The experiment was conducted under the sun during a hot summer day, and the performance of the green roof is compared with a control model, which is a bare reinforced concrete roof. The result shows that for a day with an average dry bulb temperature of 34.27 °C, the average dry bulb temperature of the room with a bare reinforced concrete roof is 31.15 °C whereas the room with a green roof installed on top has an average dry bulb temperature of 27.22 °C, almost 4 °C lower than that of the former one. Moreover, the roof thermal transfer value (RTTV) for both roof models was computed by the author, as shown in Table 2.2, to compare the difference in their performance in terms of RTTV value.

Table 2.2: Comparison of The RTTV Value for Reinforce Concrete Roof and Green Roof (Pandey, Hindoliya and Mod, 2013).

Roof type	Peak heat transfer (W)	Area (m ²)	Peak RTTV (W/m ²)	Reduction (%)
Bare reinforced concrete roof	16.8	1	16.8	-
Green roof	3.0	1	3.0	73.8%

Table 2.2 shows that there is a remarkable 73.8% decline in RTTV value for the green roof. Both the reduction in room average temperature and RTTV value for the green roof model compared to the bare reinforced concrete roof model provide very strong evidence that green roofs are very effective in reducing the heat flux transfer into the space directly below the roof.

Furthermore, Pandey, Hindoliya and Mod (2013) also suggest that the foliage height of the plant plays an important role in preventing heat flow into the space under the roof. Higher foliage height can block more solar radiation from heating the soil surface, which may inadvertently reduce the plants cooling effect of evapotranspiration. Evapotranspiration dissipates portions of the heat flux on the surface and releases the latent heat into the atmosphere (Bevilacqua, 2021). Hence, higher foliage height can prevent more heat flux from being transferred into the attic space.

2.3.2 Lightweight Foam Concrete (LFC) Roof Tile

LFC is a prevalent building material dubbed many names, such as lightweight cellular concrete (LCC), foamed concrete, and low-density cellular concrete (LDCC). As the name implies, LFC is low in weight and density, which is possible to achieve by adding a foaming agent to the cement mix (Claisse, 2016). According to Ramamurthy, Nambiar and Ranjani (2009), as cited by Kozłowski and Kadela (2018), the density of the LFC ranges from 300 kg/m³ to 1600 kg/m³ can be achieved by adjusting the amount of foaming agent to be mixed with other cement material. Furthermore, this will introduce a cellular microstructure to the concrete that can entrain 20% to as high as 50% of air within the structure,

causing it to be porous (Claisse, 2016; Kozłowski and Kadela, 2018; Bindiganavile and Hoseini, 2019). As a result, the porosity and air entrapped in the concrete cause it to be low in density compared to an RCC Concrete with the same volume. Due to its low-density property, which may be attributed to its porous characteristic, it has relatively low thermal conductivity, making it a good choice of thermal insulator material to be integrated into the cool roof design. Ramamurthy (2009), as cited by Mohd Sari and Mohammed Sani (2017), also suggested that LFC with a density range of 400 kg/m^3 to 1600 kg/m^3 can be used for insulation besides other structural purposes.

An experimental study on the thermal insulation performance of LFC as the roof tile of a cool roof system has been done by Yew et al. (2021), which successfully proved that LFC could lower the attic temperature compared to conventional roof tile. LFC with dry densities between 600 kg/m^3 and 1600 kg/m^3 has a thermal conductivity of 0.1 W/mK to 0.7 W/mK , which is 5% to 30% lower than ordinary concrete (Mohd Sari and Mohammed Sani, 2017). The density of the LFC used in the experiment is 1250 kg/m^3 and thermal conductivity of 0.61 W/mK , which is much lower than that of reinforced cement concrete (RCC) roof slab. For comparison, a typical B12.5 concrete roof slab has a density and thermal conductivity of 2400 kg/m^3 and 1.55 W/mK , respectively (Tho, Korol and Hoang, 2018). In addition, reinforced concrete with steel bars as composite material have thermal conductivity ranging from 1.43 W/mK to 2.10 W/mK , depending on the orientation and arrangement of the steel bars (Zhao et al., 2013). LFC has good thermal insulation properties due to the air pockets entrapped inside the structure.

Figure 2.6 shows the experimental results obtained by Yew et al. (2021), for their roof models. Among their experiment roof models, two models, the metal roof and the LFC roof are compared in this context.

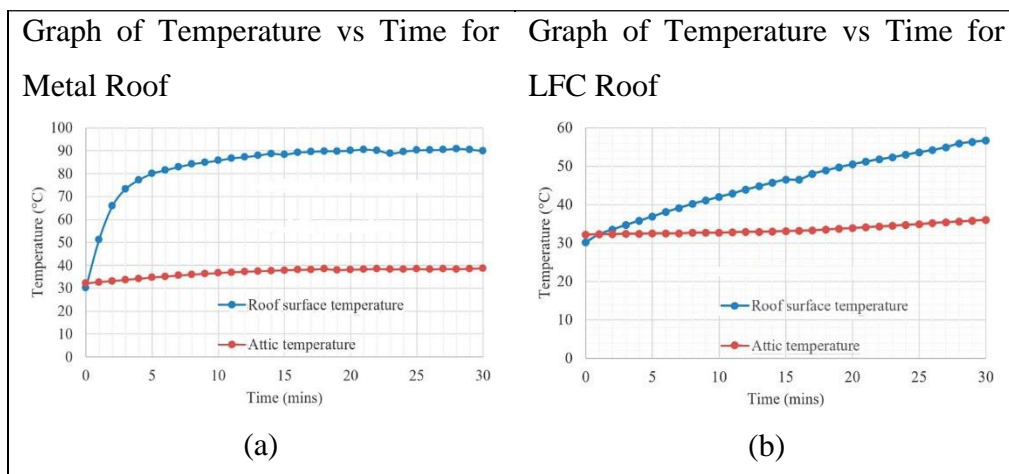


Figure 2.6: Comparison Between the Performance of (a) Metal Roof and (b) LFC Roof (Yew et al., 2021).

Based on Figure 2.6, the surface temperature of the metal roof can reach as high as 90.8 °C, whereas the maximum surface temperature of LFC is only 56.7 °C, which is 34.1 °C lower than that of the metal roof. Furthermore, the roof model with LFC also has the lowest attic temperature of 36.0 °C, about 2.6 °C lower than the highest attic temperature of the model with a metal roof, which reached 38.3 °C (Yew et al., 2021). The findings show that a cool roof with tile made of LFC can block a substantial amount of solar energy from transferring into the attic and, eventually the living space.

Table 2.3 shows the difference between the average increment rate of attic temperature for the metal roof and the LFC roof.

Table 2.3: The Average Increment Rate of Attic Temperature for Various Roof Tiles (Yew et al., 2021).

Roof tile	Average increment rate of attic temperature (°C/min)
Metal deck	0.2167
LFC	0.1267
LFC with MAC	0.0300
LFC with MAC and S-P Fs	0.0167

The average increment rate of attic temperature is 0.2167 °C/min and 0.1267 °C/min for the metal roof and LFC roof, respectively. As expected, the LFC roof model has a lower rate, which is 0.09 °C/min (41.5%) lesser. The lower rate indicates a smaller gradient, which means that the attic temperature has a smaller increment at a given time. In other words, it is harder for the solar heat to be transferred into the attic region due to the high thermal insulation property of the roof material.

However, a cool roof design with only LFC as a substitute for conventional roof material is not enough to significantly affect attic temperature reduction. Thus, other features such as the MAC and fans can be integrated with the cool roof design to prevent more heat from penetrating the attic space (Yew et al., 2021). Based on Table 2.3, the LFC cool roof fitted with a MAC and S-P Fs can achieve a comparably low average rate of attic temperature of 0.0167 °C/min, 92.3% lower than that of the regular metal roof design.

Since LFC is known for its characteristic of low thermal conductivity, low energy consumption, high manufacturability, cheap production cost, and lightweight, it is becoming more recognized in the building industry over the past few years (Bindiganavile and Hoseini, 2019). Moreover, it is also considered a sustainable and environmentally friendly material because the cement can be replaced with 30% - 70% fly ash to fulfil the waste utilization strategy and reduce density (Ramamurthy, Nambiar and Ranjani, 2009).

2.3.3 Active Moving Air Cavity (MAC)

MAC, also known as a solar roof collector, is a channel installed under the roof deck to act as a heat barrier and prevent the heat energy from solar radiation from transferring through the roof deck, causing temperature rise in attic space and jeopardising indoor thermal comfort. This is done by channelling the hot air out of the cavity passively or actively.

Passive heat removal by the MAC without force convection is possible due to the buoyancy effect (Yew et al., 2018). The buoyancy effect is produced by the difference in density between hot air and cold air. Hot air has a lower density as the air molecules are arranged further away from each other; cold air has a higher density as the air molecules are arranged closer to each other. Thus, hot air will rise while cold air will fall (Bergman et al., 2011).

However, the buoyancy effect is not present if the MAC is lied flat horizontally. Instead, a minimal angle is needed for the MAC to be tilted to promote the buoyancy effect in order to ventilate out the heat passively (Lee et al., 2009). Lee et al. (2009) also have established that the steeper the MAC is tilted, the faster the airflow velocity in the channel, and hence more heat will be ventilated out from it, as shown in Figure 2.7.

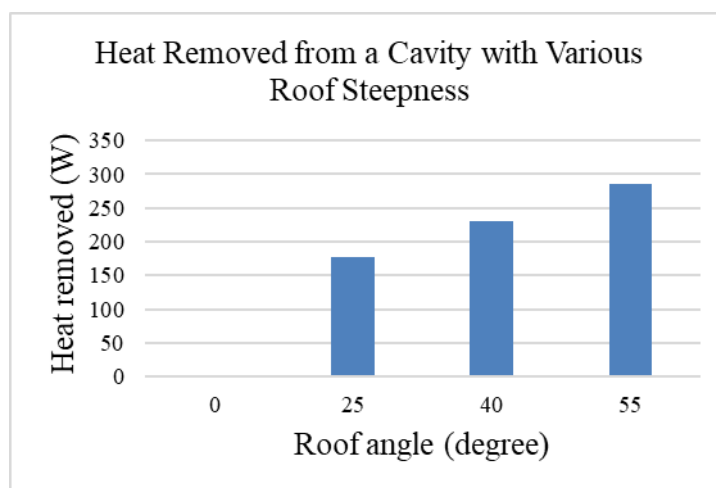


Figure 2.7: Heat Removed from a Cavity with Various Roof Steepness (Lee et al., 2009).

The result from an investigation done by Hirunlabh et al. (2001) also supports that a higher inclination of the MAC will induce a faster airflow rate, but there is no notable increase when the tilt angle exceeded 60° . Similarly, Khedari, Hirunlabh and Bunnag (1996) also studied the optimum tilt angle for MAC and recommended that 30° inclination is ideal and able to generate a ventilation rate of as high as 0.15 m/s per unit area for a cavity length of 100 cm due to the buoyancy effect.

Other factors influencing the natural airflow rate in the MAC include dimension. According to Lee et al. (2009), the natural ventilation rate of a cavity with a dimension of $90\text{ mm} \times 30\text{ mm}$ yields 0.47 m/s, which is higher than a bigger cavity dimension of $180\text{ mm} \times 30\text{ mm}$ with only 0.35 m/s of airflow rate achieved. This is because smaller cavity dimensions can reach a higher surface temperature since it has a shorter perimeter length that can transfer conduction heat faster and has a shorter distance between adjacent surfaces, which helps radiate more heat to one another. Higher surface temperature promotes more

buoyancy force that results in higher natural ventilation velocity and subsequently exhausts more heat to the surrounding. Therefore, a square shape cavity is recommended rather than a rectangular cavity to design an efficient MAC.

On the other hand, an active MAC can be produced by incorporating S-P Fs at the inlet of the cavity tube. The purpose of integrating the solar-power fans is to induce a higher airflow rate so that the heat in the cavity can be rejected out to the atmosphere more effectively, hence hindering the heat from transmitting into the attic (Yew et al., 2017). It is also energy efficient as the system can be powered by sunlight on sunny days and does not require human interference since it will automatically turn on with the presence of solar radiation. Thus, this system is considered automated and spontaneously provides ventilation to cool down the cavity when needed (Yew et al., 2017).

As a comparison between the effectiveness of passive and active moving air cavity in removing heat, the experiment carried out by Khedari et al. (2002) is reviewed. Based on their findings, a MAC can achieve an airflow rate of a maximum of 250 m³/h with the additional ventilation from S-P Fs. In contrast, only a maximum of 100 m³/h is achievable without S-P Fs where the dimension and inclination of the cavity are constant with the former. In addition, Khedari et al. (2002) also added that the average temperature difference in the cavity is lower with the integration of solar-power fans compared to the conventional model that solely relies on natural convection. This further suggests that the MAC with solar-power fans can exhaust heat out to the atmosphere more effectively by increasing the airflow ventilation rate.

CHAPTER 3

METHODOLOGY AND WORK PLAN

3.1 Introduction

The cool roof system designed for this project consists of several components with thermal insulation properties to achieve passive and active cooling effects. The passive cool roof components comprised an LFC roof slab with vegetation planted on top to resemble an extensive green roof system. The targeted density for the LFC was 1250 kg/m^3 . Furthermore, a MAC made of several aluminium tubes assembly was installed under the LFC roof slab with an inclination angle of 30° to generate natural ventilation passively with buoyancy force. On the other hand, in order to obtain active cooling effects, seven solar-power fans were fitted at the inlet of the tubes for active ventilation. All the components were used to design five different roof models, which are all inclined at 30° but each with a different number of features integrated. The components for each roof model are summarized in Table 3.1.

Table 3.1: Components for Each Roof Model.

Roof Model	Components
I	Reinforced concrete roof slab
II	LFC roof slab
III	LFC roof slab, MAC
IV	LFC roof slab, active MAC fitted with S-P Fs
V	LFC roof slab, active MAC fitted with S-P Fs, vegetation layer

The experiment models consist of the cool roof fixed on top of an attic model made of an acrylic box so that the performance of different cool roof models could be evaluated by measuring the attic temperature reduction. K-type thermocouples were used to measure the temperature at different points of the cool roof model: the roof surface, attic space, ambient air, and inside the MAC. Two 500 W spotlights were used to shine on the cool roof for 30 minutes to

simulate the solar radiation condition. The temperature at each point was recorded for every 1-minute interval. The experiment was repeated for five roof models. Figure 3.1 demonstrates the experiment's approach in the form of a flow chart.

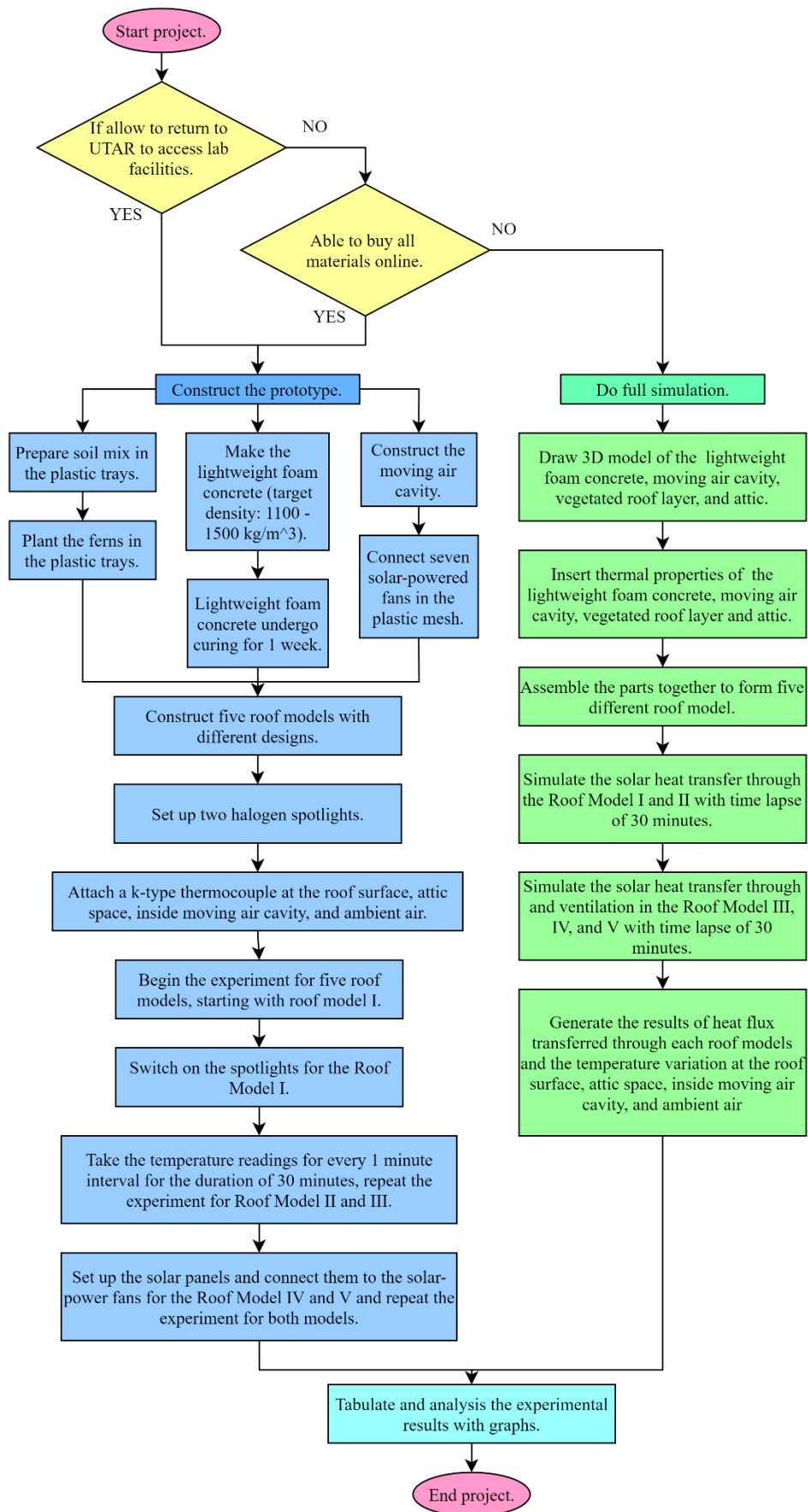


Figure 3.1: The Experiment Process Flow Chart.

3.2 Roof Model Designs

Five roof models were proposed for the experiment and the roof components involved in the design were reinforced concrete roof slab, LFC roof slab, MAC, S-P Fs, and vegetation layer planted with ferns and wormwood. The components were integrated into each roof model in stages to compare their thermal insulation performance for attic temperature reduction in the experiment. For instance, Roof Model I had a reinforced concrete roof slab; Roof Model II replaced the reinforced concrete roof slab with an LFC roof slab; Roof Model III had an additional component to Roof Model II, which was a MAC under the LFC roof slab; Roof Model IV would add the S-P Fs to the existing design of Roof Model III for active cooling purpose; lastly, for Roof Model V would integrate all the cool roof components with another accessory which was a vegetation layer planted with ferns and wormwood to simulate an extensive green roof system. The schematic design for each roof model is illustrated in Figure 3.2, with the components being labelled. All the roof models are inclined at 30°.

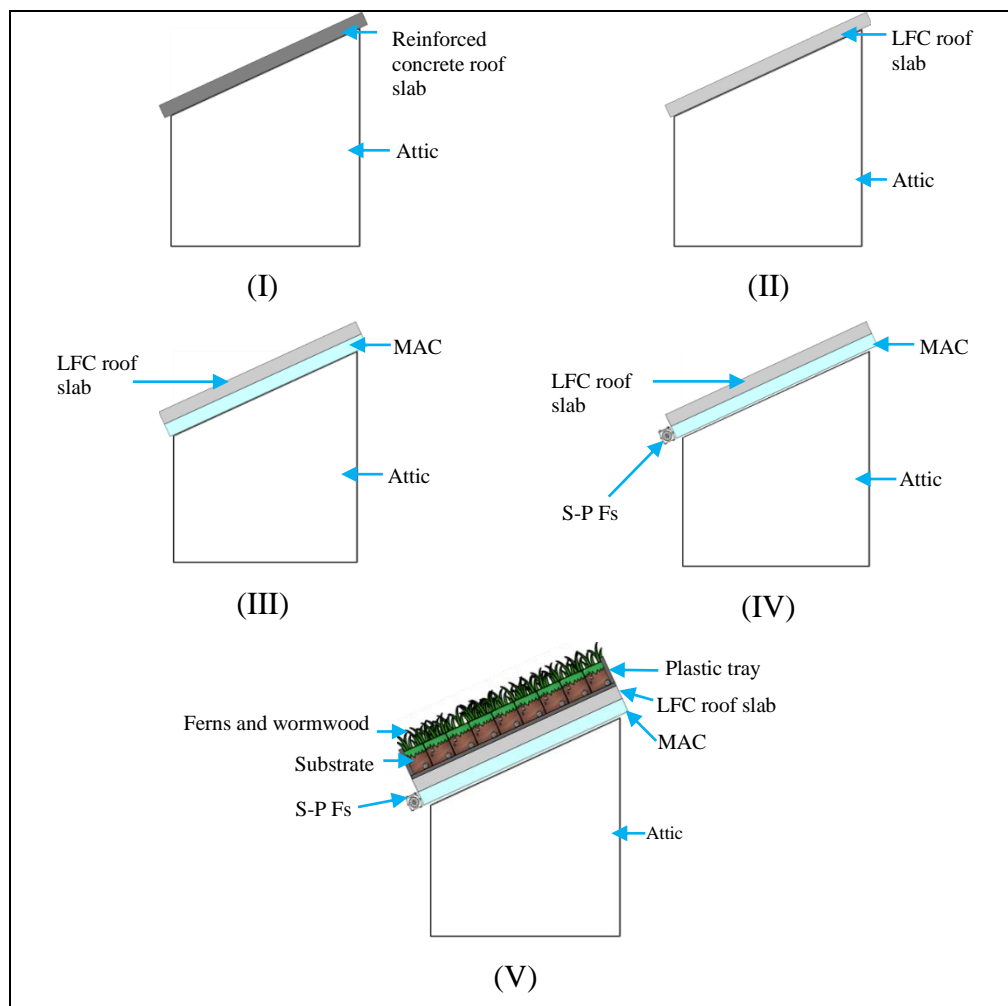


Figure 3.2: Roof Models I, II, III, IV and V.

3.2.1 Roof Model I (Reinforced Concrete Roof Slab)

The Roof Model I was constructed with a reinforced concrete roof slab with a proposed dimension of $450 \text{ mm} \times 350 \text{ mm} \times 50 \text{ mm}$, as shown in Figure 3.2 (I). This roof model would act as a control variable since it is commonly built for most buildings in Malaysia. The thermal insulation performance of other roof models will compare against this first design.

3.2.2 Roof Model II (LFC Roof Slab)

As depicted in Figure 3.2 (II), the Roof Model II would swap the reinforced concrete roof slab from Roof Model I to an LFC roof slab with the dimension of $450 \text{ mm} \times 350 \text{ mm} \times 50 \text{ mm}$. It was expected that this LFC slab would reduce the heat flux into the attic compared to the reinforced concrete roof slab in Roof Model I because it has a lower thermal conductivity value. LFC has an expected

thermal conductivity from 0.38 W/mk to 0.62 W/mk for density ranging between 1100 kg/m³ and 1500 kg/m³, whereas reinforced concrete generally has a thermal conductivity of around 1.5 W/mk. In other words, LFC is a good thermal insulator whereas reinforced concrete is a thermal conductor and the attic temperature reduction performance of the former was expected to be better. Thus, Roof Model II was expected to show better results with lower attic temperatures than Roof Model I.

3.2.3 Roof Model III (LFC Roof Slab with MAC)

A MAC was installed under the LFC roof slab for the third design, as illustrated in Figure 3.2 (III). It has the same dimension as the roof slab, which is 450 mm × 350mm × 50 mm, and the cavity is divided into seven tube sections. Since the roof model is inclined at 30°, the buoyancy effect will induce passive ventilation and the performance in heat rejection will be tested in the experiment.

3.2.4 Roof Model IV (LFC Roof Slab with Active MAC Fitted with S-P Fs)

Referring to Figure 3.2 (IV), the components in Roof Model IV were identical to Roof Model 3 with the inclusion of seven solar power fans to induce active ventilation and the efficiency can be compared. Since the airflow was actively induced by the S-P Fs, the ventilation rate will be higher than Roof Model III with no solar-power fans installed and solely rely on natural ventilation induced by buoyancy force. Another advantage of S-P Fs is that the energy consumed is green and renewable so that no extra electricity is consumed from the power grid.

3.2.5 Roof Model V (LFC Roof Slab Topped with Vegetation Layer with Active MAC Fitted with S-P Fs)

The final design, Roof Model V, as illustrated in Figure 3.2 (V), comprises all the combined components. This model was a simplified replica of a comprehensive green roof system so that the performance of a green roof in attic temperature reduction and cooling effect could be investigated. A layer of vegetation planted with fern and wormwood was fixed on top of the roof slab with some shear barrier to provide additional support and prevent sliding of the

vegetation layer. The vegetation layer acted as a thermal insulator that prevents incident solar radiation heat from transferring into the attic space directly moving the attic space as the thermal conductivity could be as low as 0.23 W/mK.

3.3 Roof Model Components

The prototype of the cool roof system consisted of different components: the vegetation layer, LFC roof slab, MAC, and S-P Fs. The cool roof was installed on the attic model, which will be made of an acrylic box of 5.00 mm thickness. As shown in Figure 3.3, the base of the attic was designed to be 355.00 mm × 340.00 mm and the roof attachment surface has an area of 409.94 mm × 340.00 mm with an inclination of 30°.

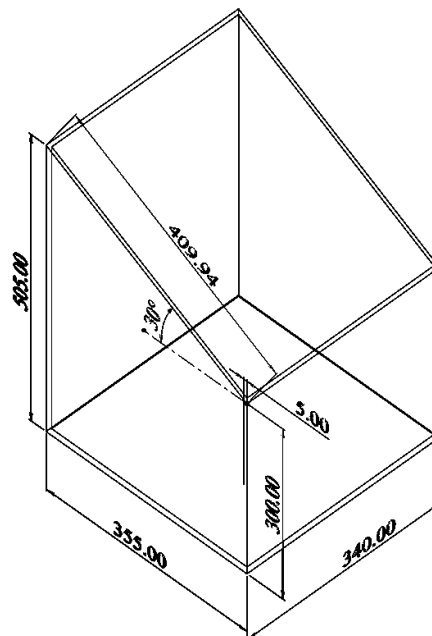


Figure 3.3: The Dimension of Attic in Millimeters.

3.3.1 Vegetation Layer

The vegetation layer was produced by planting fern and wormwood in a wood tray with 100 mm of the substrate layer as shown in Figure 3.4.



Figure 3.4: Wood Tray.

Fern and wormwood were chosen because they have a high foliage layer, which can provide more shading from the sun. Besides, they also have a fast growth rate that can quickly cover up the roof area and become a dense shrub layer with more transpiration for the cooling effect. Also, the fern is one of the CAM plants that can survive the roof's harsh and dry climate. All these characteristics are the perfect candidate for the green roof plant. Most importantly, fern and wormwood are widespread and easily found in Malaysia.

The 100 mm substrate layer consisted of a mixture of soil, organic matter, and sand. The ratio of soil to organic matter to sand was 3:2:1. Other than that, since the roof is angled at 30°, construction waste materials - gravels were added to prevent substrate run-off caused by water (Hui, 2011). Figure 3.5 illustrates the cross-sectional view of the vegetation layer. The substrate layer was expected to have a thermal conductivity of 0.23 W/mK (Pandey, Hindoliya and Mod, 2013).

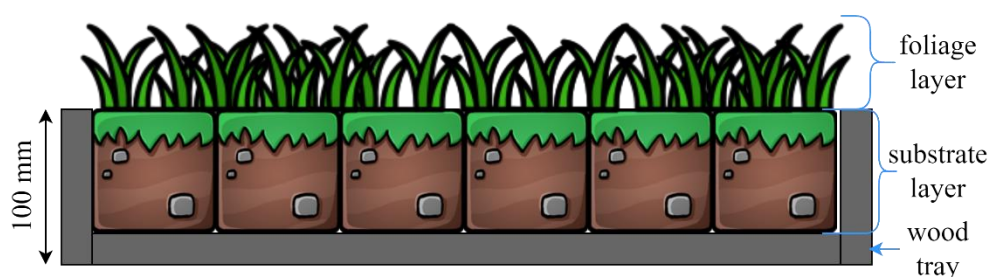


Figure 3.5: The Schematic Diagram of The Vegetation Layer.

According to Hui (2011), an anti-shear barrier or horizontal strapping is needed for vegetated roofs with a pitch angle of 30°. This is because the shear force from the substrate is too great and requires additional support to transfer the load to the roof structure. Commonly, the soil retention system is done by dividing the roof into sections of 1 ft² (Sloped Green Roofs, 2021). Therefore, one shear barrier was attached to the roof slab in front to support the wood tray of the plant and another shear barrier was attached in the middle of the wood tray as shown in Figure 3.4, to divide the substrate into smaller cells so that the shear weight can be overcome.

3.3.2 Lightweight Foam Concrete (LFC) Roof Slab

The dimension of the LFC roof slab was 460 mm × 360 mm × 30 mm and the targeted density was 1250 kg/m³ to provide adequate strength to support the vegetation layer (Mohd Sari and Mohammed Sani, 2017). Although the lower density is good for insulation, it cannot be too low because it needs to support the weight of the soil medium and plant on top.

The raw materials needed were cement, sand, foam, and water (Bindiganavile and Hoseini, 2019). The water/cement ratio and sand/cement ratio were determined as 1:0.6 and 1:1 respectively. Thus, 3 kg of water and 1.8 kg of cement and sand each were used for the mix. To determine the amount of foam needed to add to the base mix, equation (3.1) was used (Ravindra and Michael, 1996; Iyer, 2020).

$$F_m = B_m \times F_d \left(\frac{1}{T_d} - \frac{1}{B_d} \right) \quad (3.1)$$

Where

F_m = Foam mass, kg

B_m = Base mix mass, kg

F_d = Foam density, kg/m³

T_d = Target dry density, kg/m³

B_d = Base mix density, kg/m³

The base mix mass, foam density, and base mix density were measured at 6.6 kg, 50 kg/m^3 , and 2500 kg/m^3 respectively, so the calculated foam mass required was 0.132 kg. The foam was mixed with the base mix evenly.

Then, the cement paste was poured into a mould with a cavity area of $460 \text{ mm} \times 360 \text{ mm}$ and a depth of 44 mm until the height of 30 mm as desired by the roof slab design. Two layers of wire mesh were placed inside the cement paste. After leaving the mortar in the mould to dry for one day, it was completely hardened and removed for water curing for one week (Palmer, 2020).

The reinforced concrete roof slab was prepared in a similar manner, except no foam was added to the base mix. The water/cement ratio and sand/cement ratio were determined as 0.5:1 and 1:1 respectively, so 5 kg of water and 10 kg of cement and sand each were mixed together. The thermal conductivity of a reinforced concrete slab was expected at around 1.5 W/mk, whereas for LFC, the roof slab would be approximately 0.38 W/mk to 0.62 W/mk for density ranging between 1100 kg/m^3 and 1500 kg/m^3 (Mohd Sari and Mohammed Sani, 2017).

3.3.3 Moving Air Cavity (MAC)

The MAC was installed under the LFC roof slab for the Roof Model III, IV, and V. The MAC has a dimension of 350.00 mm in width and 450.00 mm in length. The cavity is divided into seven tube sections as shown in Figure 3.6.

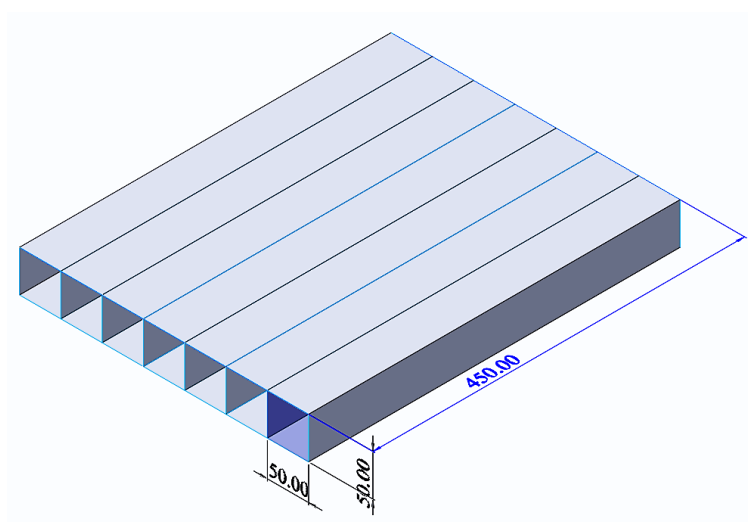


Figure 3.6: Dimension of MAC in Millimeters.

The outer surface of the MAC was covered with aluminium sheets while the divider of the seven tube sections was made of aluminium foil, which materials are shown in Figure 3.7 respectively.

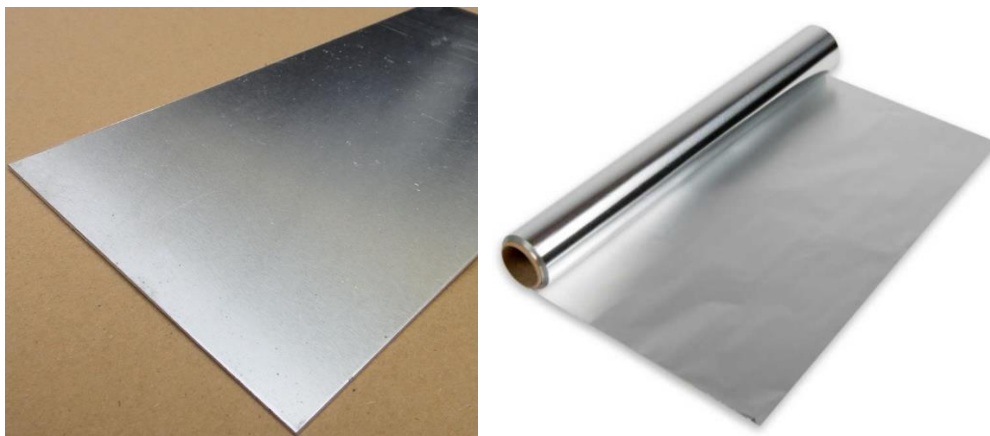


Figure 3.7: Aluminium Sheet (Left) and Aluminium Foil (Right).

Steel rods were used to build the structural backbone of the MAC whereas the wire mesh as shown in Figure 3.8 was used to form the divider of the MAC. The aluminium sheets were attached to the steel rod frame to form the outer shell whereas aluminium foils were attached to the wire mesh to form an enclosed divider.



Figure 3.8: Wire Mesh.

3.3.4 Solar-Powered Fans (S-P Fs)

Each inlet of the MAC was fitted with S-P Fs. Seven S-P Fs were needed since there are seven tube inlets. The installation of S-P Fs for the Roof Model IV and V can introduce active airflow which will theoretically remove more heat into

the atmosphere and make the attic space cooler than other designs. The MAC was sectioned into seven square tubes to ensure laminar flow when the air velocity is introduced at the inlets. Furthermore, S-P Fs utilized green and renewable energy so that electricity is conserved.

3.4 Experiment Set-up

Two 500 W spotlights that simulate the condition of the sunlight were set up at a distance of 40 cm from the roof surface, projecting light perpendicularly on it. Four k-type thermocouples were used to measure the temperature at different points of the roof model. The measurements taken were roof surface temperature (T1), inside attic temperature (T2), ambient temperature (T3) which was 15 cm from the centre of the roof surface, and inside MAC temperature (T4). The k-type thermocouples were attached at the centre of each component, as illustrated in Figure 3.9. Aluminium tapes were used to stick the thermocouple on the roof surface to measure T1.

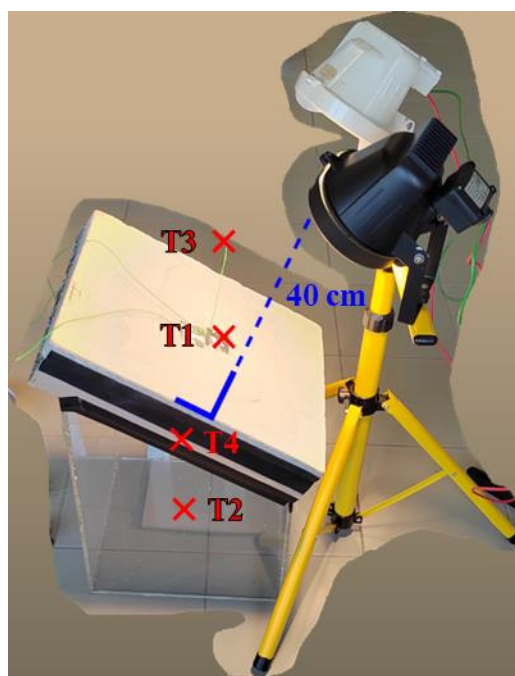


Figure 3.9: Set Up of Roof Model.

However, Roof Model V had a layer of vegetation placed atop the LFC, so another thermocouple was used to measure the soil temperature (T5).

CHAPTER 4

RESULTS AND DISCUSSION

4.1 Roof Model I (Reinforced Concrete Roof Slab)

The first roof model, which was merely covered with a reinforced concrete roof slab, acts as a base model of the experiment. The measured result of the increasing temperature in 30 minutes of the roof surface, attic, and ambient is presented in a temperature graph against time as shown in Figure 4.1.

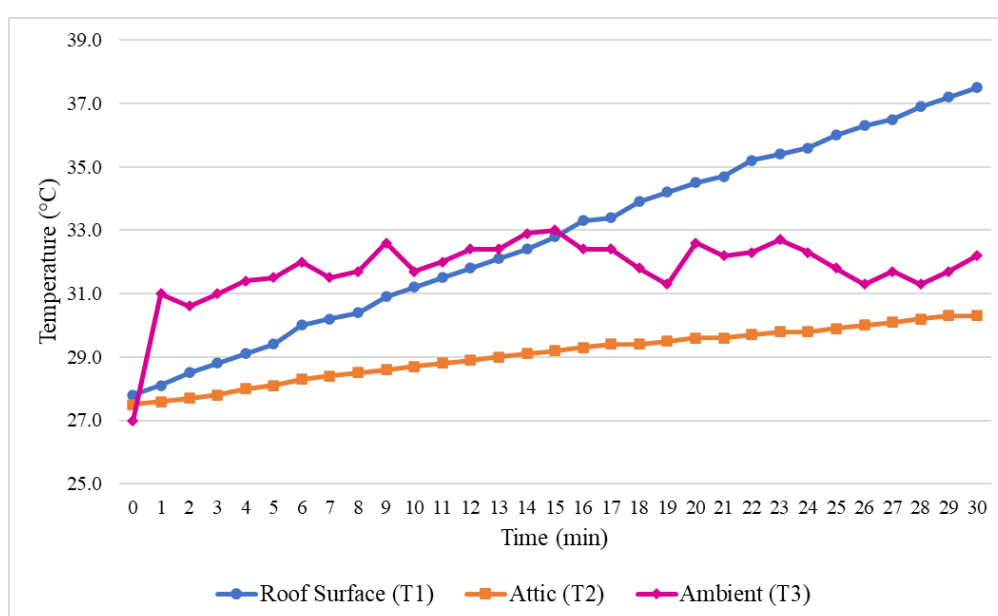


Figure 4.1: Graph of Temperature (°C) Versus Time (min) for Roof Model I (Reinforce Concrete Roof Slab).

Based on Figure 4.1, the initial ambient temperature at 0 minutes was 27.0 °C and then increased sharply to 31.0 °C when the spotlight was turned on for 1 minute and reached a peak temperature of 33.0 °C. This condition was an experimental replica of the sunny day atmosphere in Malaysia, which has an average maximum temperature of 32.0 °C in the afternoon (Tang and Chin, 2017a). It was averaged at 31.8 °C for 30 minutes during the experiment.

Besides, it was observed that the roof surface temperature and attic temperature kept increasing steadily throughout the 30 minutes duration of the experiment. The maximum temperature of the roof surface and attic was 37.5 °C

and 30.3 °C, respectively. The hot attic temperature will sooner heat up the building occupant space. Unfortunately, 30.3 °C is considered hot and uncomfortable for the dwellers because the preferred temperature for building thermal comfort is between 24 °C and 26 °C, according to the Malaysian Standard 1525. Therefore, the roof design has to be improved by integrating passive and active cool roof components.

4.2 Roof Model II (LFC Roof Slab)

The second roof model replaced the reinforced concrete in the base model with the LFC roof slab and the result is also shown in a graph of temperature against time as in Figure 4.2.

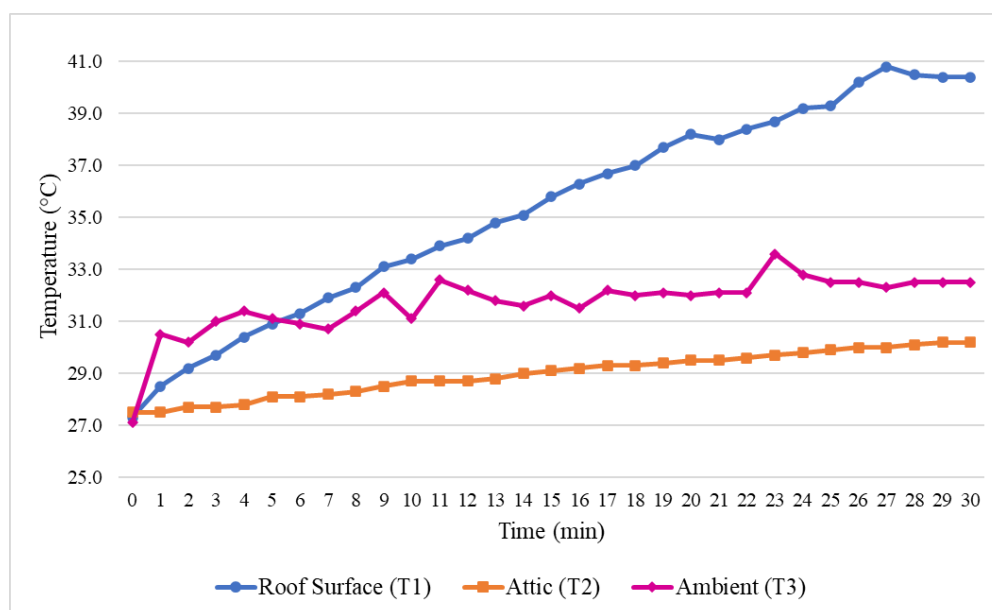


Figure 4.2: Graph of Temperature (°C) Versus Time (min) for Roof Model II (LFC Roof Slab).

The average and maximum ambient temperature during the experiment of roof model II were 31.7 °C and 33.6 °C respectively, which is almost the same as the condition in roof model I experiment.

By referring to Figure 4.2, the roof surface temperature and attic temperature exhibit a similar trend compared to the base model as they both rose gradually. However, the peak roof surface temperature was 40.8 °C, which is 3.3 °C higher than the base model. Despite the higher roof surface temperature

of the second roof model, the attic temperature was able to achieve a 0.1 °C lower maximum temperature than the base model at 30.2 °C.

This showed the effectiveness of LFC in preventing more heat from penetrating into the attic. This is because the thermal conductivity of the LFC is lower than that of the reinforced concrete. A typical reinforced concrete has a thermal conductivity of 1.5 W/mk. In contrast, LFC is between 0.38 W/mk and 0.62 W/mk for density ranging between 1100 kg/m³ and 1500 kg/m³, which is less than half of the reinforced concrete to its porous property (Mohd Sari and Mohammed Sani, 2017).

4.3 Roof Model III (LFC Roof Slab with MAC)

Next, the MAC was retrofitted to the roof model II by installing it under the LFC roof slab to produce roof model III. Similarly, the result of the performance of this roof model is plotted in a graph of temperature against time shown in Figure 4.3.

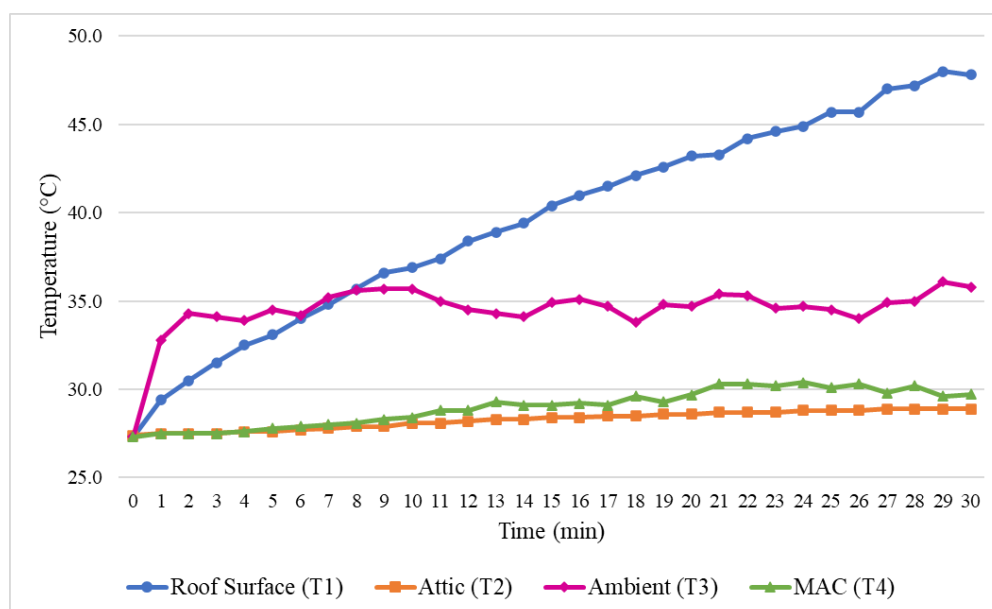


Figure 4.3: Graph of Temperature (°C) Versus Time (min) for Roof Model III (LFC Roof Slab with MAC).

In the experiment of this roof model, the ambient condition was slightly hotter than in the previous two experiments, with a maximum ambient temperature of 36.1 °C and averaging at 34.5 °C.

Based on Figure 4.3, it can be observed that the roof surface temperature still increased regularly, resembling the trend in roof models I and II. It reached a maximum temperature of 48.0 °C. The hotter ambient condition might have caused the maximum roof surface temperature to be 7.2 °C more than roof model II and 10.5 °C more than roof model I.

However, the trend of the attic temperature was different from those in roof models I and II since the increment was marginal. In spite of the higher roof surface temperature, the maximum attic temperature was able to maintain at a lower temperature than roof model II. The maximum attic temperature was 28.9 °C, 1.3 °C lower than roof model II and 1.4 °C lower than roof model I. This may be attributed to the presence of the MAC above the attic, which effectively acts as an insulation that blocks the heat being transferred from the roof directly into the attic. Besides that, it applies the law of natural convection to ventilate out heat transferred from the roof to the channels of the MAC.

According to Figure 4.3, the temperature of the MAC was higher than the temperature in the attic after 5 minutes of the experiment. Initially, the temperature of both attic and MAC was about the same. Then, the temperature in the MAC exceeded the attic temperature after 5 minutes of exposure to the spotlight and reached a maximum temperature of 30.4 °C at the time of 24 minutes, 1.5 °C higher than the maximum temperature of the attic. This again proved that the MAC is able to keep the attic cooler by channelling the heat transferred from the roof to the cavity out to the atmosphere, hence less heat gain in the attic.

The remarkable contribution of the MAC to attic temperature reduction is due to the optimum design assimilating ideas from different references. For instance, the roof model had a steepness of 30° to optimize the ventilation rate (Khedari, Hirunlabh and Bunnag, 1996). Also, the cavity was evenly divided into square sections instead of letting it be a rectangular cavity without any division was designed on purpose to promote better ventilation as well. By dividing the cavity into square sections, the cross-sectional area is smaller, which promotes heat conduction and radiation within the cavity surfaces, hence achieving greater surface temperature that enhances the heat exhaustion rate (Lee et al., 2009).

4.4 Roof Model IV (LFC Roof Slab with Active MAC Fitted with S-P Fs)

The fourth roof model had S-P Fs attached to the inlet of the MAC for an active cool roof design. As shown in Figure 4.4, the graph of temperature against time was plotted to illustrate the cooling performance of the roof model IV.

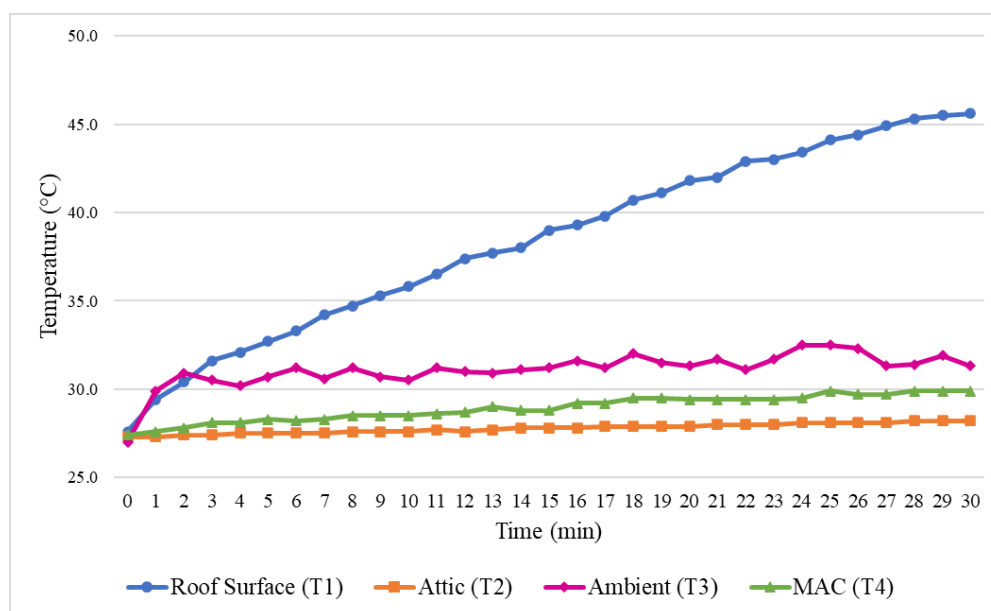


Figure 4.4: Graph of Temperature (°C) Versus Time (min) for Roof Model IV (LFC Roof Slab with Active MAC Fitted with S-P Fs).

The maximum ambient temperature recorded for this experiment was 32.5 °C while the average was 31.1 °C. Thus, the ambient condition was similar to that of the experiment on roof models I and II.

As shown in Figure 4.4, it is noted that the trend of the roof surface and attic temperature was identical to roof model III, with the roof surface temperature exhibiting gradual increment while the attic temperature increased slightly. The maximum roof surface temperature was 45.6 °C, while the maximum attic temperature was slightly lower than that in roof model III, which is 28.2 °C. The attic temperature of roof model IV was 0.7 °C cooler than the attic temperature of roof model III and 2.1 °C cooler than that of roof model I. This may be attributed to the active ventilation by the S-P Fs since more heat was forced out into the atmosphere. It is also observed that the maximum roof surface temperature was 2.4 °C lower than the roof model III without S-P Fs at

the MAC. This is due to the active ventilation provided by the S-P Fs that exhaust more heat (Khedari et al., 2002).

The S-P Fs induced more airflow in the cavity, causing a lower temperature in both the cavity as well as the attic (Khedari et al., 2002). Furthermore, the MAC temperature was higher than in the attic throughout the experiment. The maximum temperature in the MAC was 29.9 °C, which was 0.5 °C lower than in roof model III. This justified that the S-P Fs contributed to the work to remove more heat trapped in the MAC, causing cooler temperature.

4.5 Roof Model V (LFC Roof Slab Topped with Vegetation Layer with Active MAC Fitted with S-P Fs)

The last roof model was designed by adding another component to the previous roof model, which was a vegetation layer. It was an experimental representation of a green roof. Likewise, the temperature rose in each roof model component was plotted against the time as displayed in Figure 4.5.

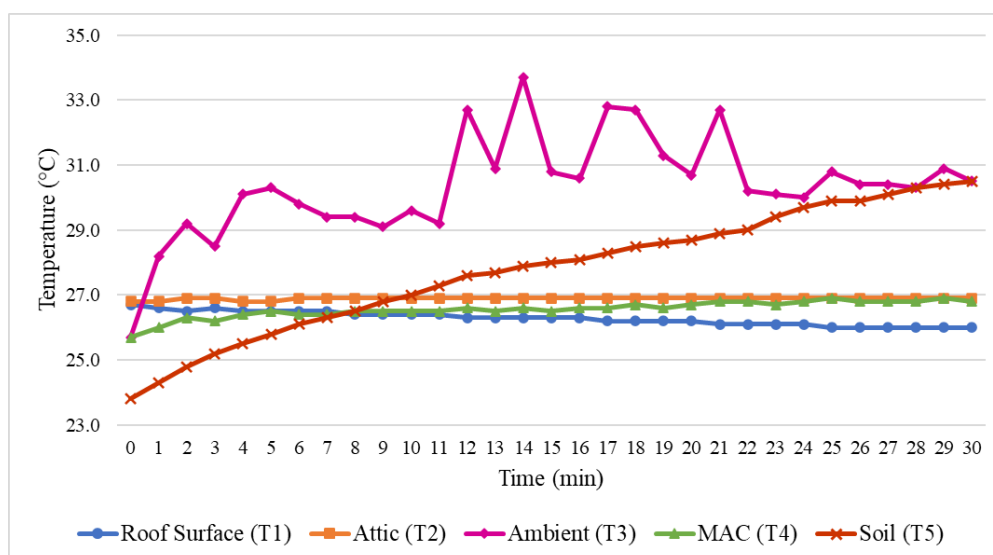


Figure 4.5: Graph of Temperature (°C) Versus Time (min) for Roof Model V (LFC Roof Slab Topped with Vegetation Layer with Active MAC Fitted with S-P Fs).

According to Figure 4.5, the trend of the ambient temperature showed greater fluctuation than in the previous models due to the coverage of the foliage layer on the thermocouple probe. The probe was positioned 15 cm from the soil

surface but the highest foliage at the centre was 45 cm. It is noted that the ambient condition was cooler for the time before 11 minutes and then suddenly increased. This is because leaves were covering the thermocouple probe, shielding it from the direct light from the lamps. After 11 minutes, the leaves started to wilt, causing the spotlight to project directly to the thermocouple probe and causing a maximum temperature of 33.7 °C at the time of 14 minutes. The mean ambient temperature recorded was 30.4 °C, the lowest amongst other roof models experiment. This may be attributed to the transpiration process of the foliage layer that can release heat to the surroundings (Bevilacqua, 2021). Overall, the trend of the ambient temperature showed more significant fluctuation compared to the previous roof models due to the leaves fluttering minorly, disturbing the light from the lamp shining directly on the thermocouple probe.

The soil surface temperature was also measured for this experiment and showed a steady upward trend which resembled the roof surface temperature trend in all the previous roof models. It increased from 23.8 °C to 30.5 °C. It is noted that the initial and final temperature of the soil is generally lowered than the roof surface temperature in all the previous roof models. This may be attributed to the cooling effects on the surface from the plant's transpiration process and the blocking of direct radiation from the spotlight by the thick foliage layer (Pandey, Hindoliya and Mod, 2013).

The incorporation of the vegetation layer had a great impact on the LFC roof surface and attic temperature. As exhibited by the trend of roof surface temperature and attic temperature in the blue line and orange line, respectively in Figure 4.5, there was hardly any increment in both. The highest roof surface temperature was 26.7 °C, the initial temperature. Instead of increasing the temperature, it decreased to 26.0 °C after 30 minutes, 19.6 °C and 11.5 °C lower than roof models IV and I. The dropped in the roof slab surface temperature may be caused by the active heat rejection from the MAC with solar-powered. On the other hand, the attic temperature was almost maintained at a constant level of 26.9 °C, 1.3 °C and 3.4 °C cooler than roof models IV and I respectively. The attic temperature only increased by 0.1 °C at time 3 minutes and ceased increasing. This shows the effective attic thermal reduction of the whole system incorporating vegetation layer and LFC, which are both very low in thermal

conductivity and an active MAC with high convection force rejecting the heat. Hence, less heat was being transferred to the attic

The MAC also showed less increment in its temperature. Its initial temperature was lower than in the attic at 25.7 °C, whereas the attic started at 26.8 °C. The MAC temperature had a moderately sharp increase in the first 5 minutes, then slowly reached a steady-state afterwards. The maximum temperature gained was 26.9 °C, which was the same as the maximum attic temperature and 3.0 °C lower than that in roof model IV. Furthermore, the increase in MAC temperature showed that it was actively and constantly removing heat transferred from the roof slab and preventing heat transfer to the attic. Therefore, a slight temperature decrement on the roof slab surface was observed.

The combination of the LFC roof slab with vegetation layer and active MAC had successfully maintained an almost constant cool temperature in the attic. To ensure the building occupants feel comfortable at the indoor temperature, the temperature has to be maintained at 24 °C to 26 °C (Malaysian Standard 1525, 2014). Therefore, the cool attic temperature achieved by roof model V will also keep the indoor temperature low, promoting indoor thermal comfort with minimal electricity consumption on the air-conditioning system since the cooling load can be considerably reduced.

4.6 Comparison between different roof models

For a more comprehensive comparison of the performance between different roof models, the temperature rise on each individual component of the roof structure is compared against the corresponding element in the predecessor design and base model. The results are discussed explicitly as follows with the aid of graphs of temperature against times of all the roof models.

4.6.1 Variation in Roof Surface Temperature

Figure 4.6 shows the variation in roof surface temperature for different models. Only roof model 1 was installed with a reinforced concrete roof slab whereas the rest were installed with an LFC roof slab. For the last roof model, roof model V, the vegetation layer was attached on top of the roof surface, simulating a green roof model.

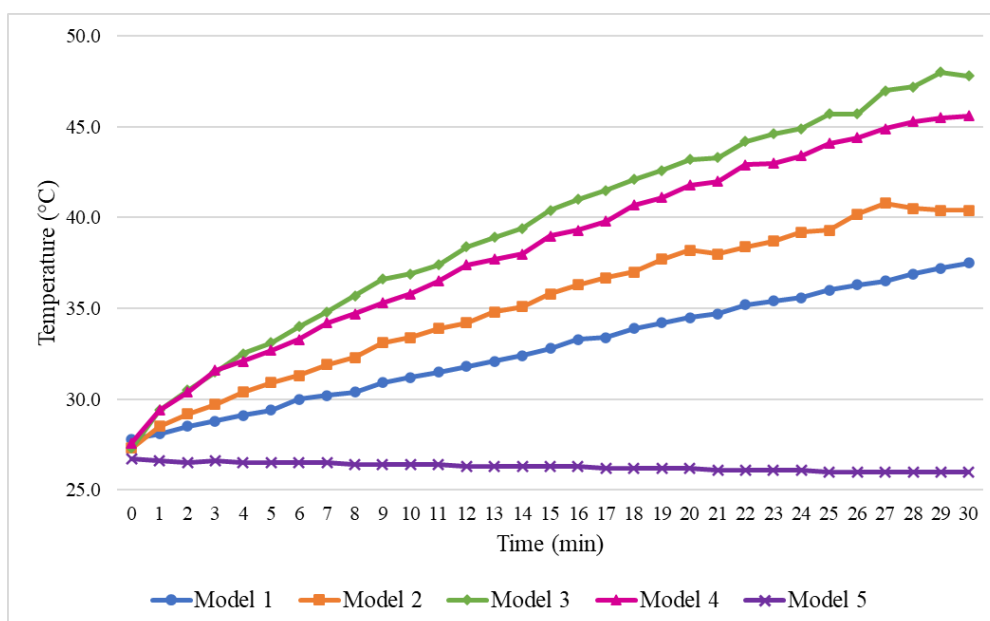


Figure 4.6: Variation in Roof Surface Temperature (°C) for Different Models.

According to Figure 4.6, the roof surface temperature on all roof models increased steadily except for roof model V which had an almost flat trend in the temperature rise. This is because roof model V had a layer of vegetation attached on top of the roof surface with thick soil and high foliage, which impeded the heat from transferring to the roof slab surface. The high foliage layer provides cooling by evapotranspiration and prevents direct heat radiation on the soil surface (Pandey, Hindoliya and Mod, 2013). In addition, the thick soil has a low thermal conductivity value which further reduces the amount of heat transferred to the roof surface. According to (Abu-Hamdeh and Reeder, 2000), soils have a thermal conductivity of 0.29 W/m K to 0.76 W/m K and the presence of organic matter in soil can further reduce its thermal conductivity. The soil mixture of the vegetation layer was composed of 3 parts soil, two parts organic matter, and 1 part sand, which made up about 30% of organic matter. The soil with 30% organic matter can have a thermal conductivity as low as 0.17 W/m K (Abu-Hamdeh and Reeder, 2000). As a result, the lightweight foam roof surface temperature remained cool without much rise in surface temperature.

4.6.2 Variation in Attic Temperature

Figure 4.7 shows the comparison between the variation in attic temperature for different roof models.

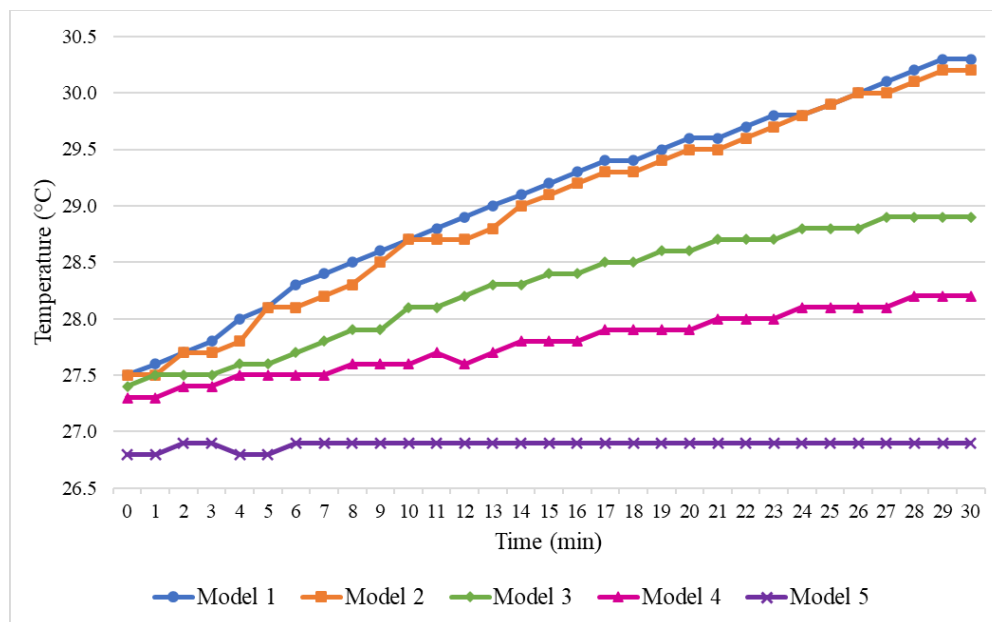


Figure 4.7: Variation in Attic Temperature (°C) for Different Models.

Based on Figure 4.7, It is observed that the attic temperature for roof models I and II had a steeper inclination, while roof models III and IV had the attic temperature increase more gradually, whereas roof model V managed to maintain the attic temperature at an almost constant level. The attic temperature of each roof model is lower than its predecessor design. This proves that each cool roof element added in the successive design had cooling effects and reduced the temperature rise in the attic.

In order to interpret the result more comprehensively, the variation in roof surface temperature and attic temperature is translated into the percentage of temperature increment and average attic temperature increment rate, which were plotted in a bar chart as shown in Figure 4.8. It is noted that the percentage of attic temperature increment corresponded to the average attic temperature increment rate as one decreased, another would follow.

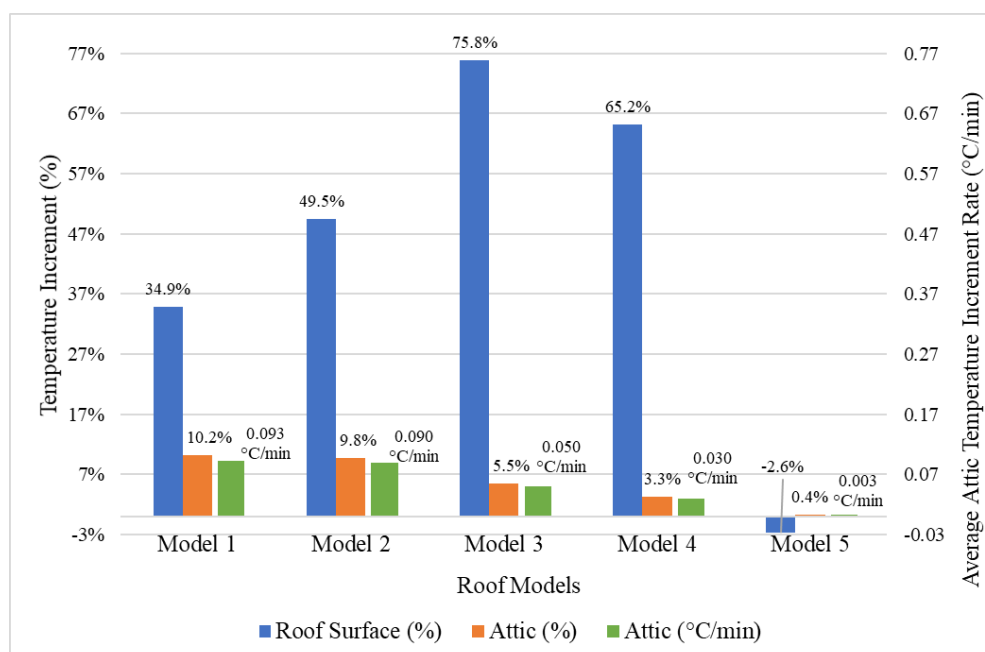


Figure 4.8: Temperature Increment (%) on Roof Surface and Attic and Average Attic Temperature Increment Rate (°C/min).

According to Figure 4.7, the difference between the maximum attic temperature of roof model I (30.3 °C) and roof model II (30.2 °C) only differs slightly by 0.1 °C. From other perspectives, the attic's temperature increment and average temperature increment rate were 10.2% and 0.093 °C/min for roof model I; 9.8% and 0.090 °C/min for roof model II, which also indicate a minor reduction. Thus, solely swapping the roof slab material into a lower density would not significantly lower the attic temperature and further improvement on the design is required. Nonetheless, it has to be pointed out that although the roof surface temperature increment of roof model II was 49.5%, which was fairly higher than that of roof model I with a 34.9% increase only, roof model II still maintained a lower attic temperature and less temperature increment rate in the attic. This is evidence that the LFC roof slab in roof model II provided a certain degree of thermal insulation since it has lower thermal conductivity than the reinforced concrete roof slab. Mohd Sari and Mohammed Sani (2017) suggested that LFCs can achieve thermal conductivity as low as 0.38 W/mk while reinforced concretes generally reach 1.5 W/mk.

A drastic decline in the attic temperature occurred for the roof model III when the MAC was added, 1.4 °C lower than the base model attic temperature. Moreover, it is worth pointing out that despite the roof surface

having the highest temperature increment of 75.8%, it achieved a lower attic temperature increment of 5.5% compared to the preceding roof models. The average attic temperature increment rate dropped to 0.050 °C/min, about 50.0% lower than roof model II. This is due to the passive cooling effect from the natural convection force induced by the inclined MAC that lets the heat flow out to the atmosphere. This is also because the MAC introduced an air gap with low thermal conductivity between the roof slab and the attic, further impeding heat transfer into the attic. According to (Dong, McCartney and Lu, 2015), the thermal conductivity of air is 0.0026 W/mK.

Roof model IV had the S-P Fs retrofitted at the inlet of the MAC which further reduced the attic temperature by 0.7 °C compared to roof model III, and by 2.1 °C compared to roof model I. The attic temperature increment in percentage and the average rate was 3.3% and 0.030 °C/min respectively, moderately lower than roof model III by 40%. The average attic temperature increment rate was 67.7% lower than that of roof model I. This indicates less heat was transferred into the attic and achieved better cooling effects that are attributed to the active work done by the S-P Fs in ventilative heat removal from the MAC.

Lastly, the final roof model showed the best thermal cooling performance as there was hardly any temperature increment. The final attic temperature was 1.3 °C lower than the prior roof model and 3.4 °C cooler than the based model. The temperature increment in the attic was 0.4% which resulted in an almost constant attic temperature throughout the exposure to the spotlight, whereas the average attic temperature increment rate was 0.003 °C/min, which was a staggering 96.77% lower than the based model and 90% lower than roof model IV. This proved that a green roof system integrated with other cool roof components: LFC roof slab and active MAC, is very effective in achieving cool attic temperature. The combination of these materials had formed very low thermal conductivity and prevented a decent amount of heat from reaching the attic.

4.6.3 Variation in MAC Temperature

Next, the temperature variation in the MAC fitted in roof models III, IV, and V are compared among each other. The increasing trend of the cavity

temperature was steady for roof models III and IV but subtle for roof model V after 3 minutes as shown in Figure 4.9.

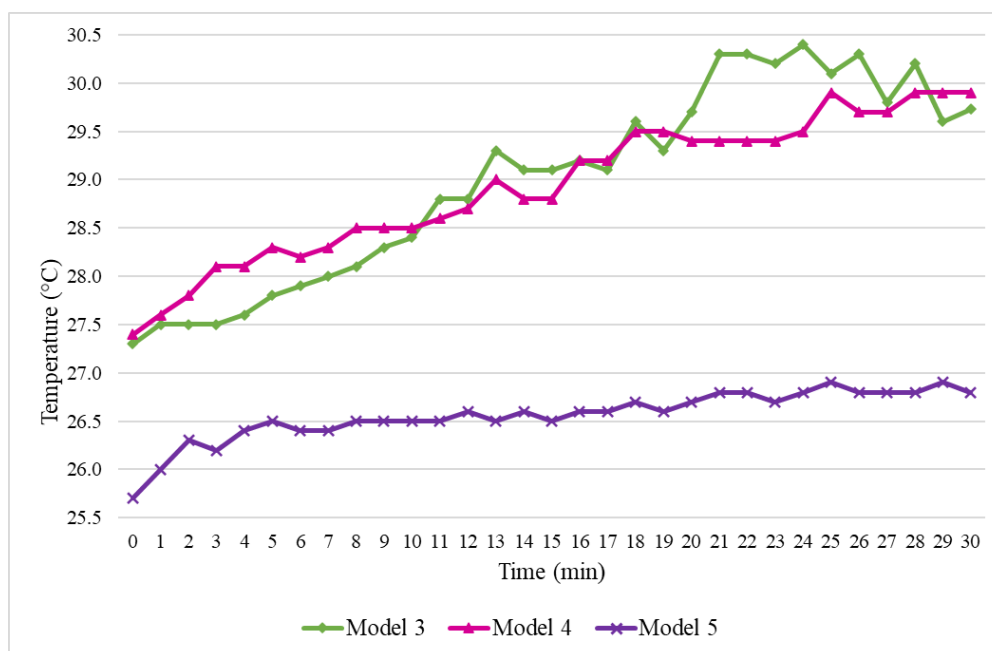


Figure 4.9: Variation in MAC Temperature (°C) for Different Models.

Comparing the trend of the MAC temperature of roof models III, and IV, it can be seen that initially from time 0 minutes to 11 minutes, the temperature of the MAC of roof model IV was greater than that of roof model III, but roof model III increased faster than roof model IV. The overall temperature increment rate for roof model III was $0.103\text{ }^{\circ}\text{C}/\text{min}$ while for roof model IV was $0.083\text{ }^{\circ}\text{C}/\text{min}$, which was 19.4% less. Therefore, the temperature in the MAC of roof model III eventually exceeded that of roof model IV after 11 minutes. The average MAC temperature for roof model III was $29.0\text{ }^{\circ}\text{C}$ whereas for roof model IV was $28.9\text{ }^{\circ}\text{C}$. The lower temperature in the MAC of roof model IV indicates a better heat removal system which may be attributed to the work done by the S-P FNs in exhausting the heat. It had successfully brought down the temperature after 11 minutes, hence a lower average temperature was obtained.

As for the MAC temperature for roof model V, the temperature initially rose sharply for the first 3 minutes, then it increased steadily afterwards. The average temperature achieved was $26.6\text{ }^{\circ}\text{C}$ and the overall rate of temperature increase was $0.037\text{ }^{\circ}\text{C}/\text{min}$, whereas it was $0.103\text{ }^{\circ}\text{C}/\text{min}$ and $0.083\text{ }^{\circ}\text{C}/\text{min}$, respectively for roof models III and IV. Based on the average temperature and

overall increment rate, they were both lower than the roof models without the vegetation layer. The roof model V's MAC overall rate of temperature increase was 55.4% lesser than that of the roof model IV, which showed the significant effect of the vegetation layer in preventing heat transfer. Besides, it was 64.1% lower than that of roof model III, which demonstrated the momentous impact of the integrating vegetation layer and S-P Fs on a cool roof system on reducing the heat transfer to the MAC and hence resulting in cooler attic condition.

4.7 Summary

A total of 5 roof models were being experimented on their performance in attic temperature reduction. The roof type of the first roof models was reinforced concrete which acted as a based model. The rest of the roof models were of improved design, integrating various passive and active cool roof elements. The passive cooling elements were an LFC roof slab, MAC, and vegetation layer whereas the active cooling element was S-P Fs. More components were added to the successive roof model and the temperature increment at different parts of the roof models was compared against the predecessor design and base model to show how much they improved in reducing attic temperature.

The LFC is a good thermal insulator with thermal conductivity of less than 1 W/mK that helps prevent heat transfer into the attic. In addition, the MAC inclined at 30° will produce convective force due to buoyancy caused by differences in the density of hot and cold air, which contributes to rejecting heat into the atmosphere, hence less heat transferred into the attic. 7 S-P Fs were utilised to remove more heat from the MAC actively by generating greater airflow rates. Lastly, the thick soil of the vegetation layer also has a low thermal conductivity that further prevented more heat transfer into the attic and the transpiration process from the high foliage provided additional thermal cooling. The thermal cooling performance of each roof model is summarised in Table 4.1.

Table 4.1: Results Summary.

Roof Model	Model I	Model II	Model III	Model IV	Model V
Roof Type	Reinforced Concrete	LFC	LFC	LFC	LFC
MAC Installed	✗	✗	✓	✓	✓
S-P Fs Installed	✗	✗	✗	✓	✓
Vegetation Layer Installed	✗	✗	✗	✗	✓
Max Roof Surface Temperature (°C)	37.5	40.8	48.0	45.6	26.7
Max Attic Temperature (°C)	30.3	30.2	28.9	28.2	26.9
Mean MAC Temperature (°C)	-	-	29.0	28.9	26.6
Attic Temperature Increment	10.2%	9.8%	5.5%	3.3%	0.4%
Mean Ambient Temperature (°C)	31.8	31.7	34.5	31.1	30.4

CHAPTER 5

CONCLUSIONS AND RECOMMENDATIONS

5.1 Conclusions

In this study, several cool roof models were designed with the aim of achieving temperature reduction in the attic. Five small scale cool roof models were built with passive thermal insulation materials and an active MAC in accordance with the objectives of this study.

The first roof model covered the attic with a reinforced concrete roof slab to serve as the base model for further comparison in terms of the improvement in successive cool roof models. Roof models II, III, IV, and V replaced the conventional reinforced concrete with passive and active cool roof elements. The passive cooling elements include an LFC roof slab, MAC, and vegetation layer whereas the active cooling element was S-P Fs, whereby more components were added to the successive roof model.

The experiment was conducted by projecting two 500 W halogen spotlights right angle at each roof model and the temperature at the ambient, roof surface, attic, and MAC was measured with k-type thermocouples for 30 minutes and the variation was shown in a plot of temperature versus times for each roof model. All roof models were inclined at 30°.

After the reinforced concrete roof slab in the roof model I was converted to an LFC roof slab for roof model II, the temperature reduction of the attic was scant as it only declined by 0.1 °C, from a maximum of 30.3 °C to 30.2 °C. The attic temperature was lower because of the thermal insulation property of the LFC due to its characteristic of low density and high porosity.

Roof model III added the MAC under the LFC roof slab. The attic temperature reduction showed a significant decline in attic temperature, in which a reduction of 1.4 °C was observed, reaching a maximum temperature of 28.9 °C. This is attributed to the natural convection force produced by the buoyancy effect that ventilated the heat to the atmosphere. Besides, the air gap of the cavity introduced low thermal conductivity between the roof slab and the attic, further impeding heat transferred into the attic.

Next, roof model IV added an active element to the MAC, which was the S-P Fs. The force convection induced by the fans further reduced the attic temperature by 0.7 °C compared to roof model III, and by 2.1 °C compared to roof model I. This gave the maximum attic temperature of 28.2 °C. This proved the active work done by the S-P Fs which can exhaust more hot air out of the cavity.

Lastly, roof model V retrofitted a vegetation layer to the whole system and gave the best performance in attic temperature reduction. The maximum attic temperature was 26.9 °C, which was 1.3 °C lower than roof model IV and 3.4 °C lower than roof model I. This is because the structure of the vegetation layer constituted thick soil and high foliage layer rendering low thermal conductivity properties and additional cooling due to the evapotranspiration process from the plant. The high foliage layer also prevents direct heat radiation on the soil surface. This satisfactory result proved that roof model V was the most effective cool roof system in keeping the attic temperature low.

In conclusion, the cool roof system combining a vegetation layer, LFC, and an active MAC can significantly reduce the attic temperature rise and keep it almost constant with the initial cool temperature. The trend of the temperature increment in the attic was almost constant and the average attic temperature increment rate was 0.003 °C/min, which was 96.77% lower than roof model I and 90% lower than roof model IV.

5.2 Recommendations for Future Work

Based on the performance of the cool roof model IV, the maximum temperature of the MAC and the attic was 0.5 °C, and 0.7 °C, lower than those in roof model III, respectively. The temperature difference can be higher by installing fans with higher revolution speed instead to achieve a higher airflow rate. The 5V DC fans used in the experiment has a revolution speed was 3500 RPM and the airflow rate produced was 7 CFM. However, DC fans of the same size with a higher voltage of 12V having a revolution speed and airflow rate of at least 4000 RPM and 11.88 CFM respectively are available in the market. Since the airflow rate is higher, more heat in the MAC will be exhausted more effectively. Hence a more distinctive temperature reduction in the MAC and attic is expected.

Moreover, to obtain better results, the experiment on all roof models shall be conducted at once to ensure their initial condition is the same. Due to materials and time constrain, only one roof model was experimented with at a time. Different hours on a day and different days have different ambient conditions, which caused the initial temperature measured on various parts of the roof models to vary and be hard to control, leading to some difficulties in the comparison. Experimenting with all roof models together at once can solve this issue.

Since this experiment was conducted indoors, under controlled conditions, the surrounding factors can be ignored. Thus, using a roof model is acceptable. The study is only limited to tropical climates because only the condition of the sunny day as simulated by the spotlights was studied. Therefore, the results may not reflect the performance of the cool roofs in places with cold seasons. Besides that, the vegetation layer was a simplified model of an extensive green roof because certain layers were excluded to reduce the complexity of the prototype. Therefore, the thermal conductivity of the excluded layers is omitted in the study.

REFERENCES

- Abd Rahman, N.M., Lim, C.H. and Fazlizan, A., 2021. Optimizing the energy saving potential of public hospital through a systematic approach for green building certification in Malaysia. *Journal of Building Engineering*, 43.
- Abu-Hamdeh, N.H. and Reeder, R.C., 2000. Soil thermal conductivity effects of density, moisture, salt concentration, and organic matter. *Soil Science Society of America Journal*, 64(4), pp.1285–1290.
- Ahmed, M.S., Mohamed, A., Homod, R.Z., Shareef, H. and Khalid, K., 2017. Awareness on energy management in residential buildings: A case study in Kajang and Putrajaya. *Journal of Engineering Science and Technology*, 12(5), pp.1280–1294.
- Anon 2021. *Sloped Green Roofs*. [online] WATERPROOF! Magazine. Available at: <<https://www.waterproofmag.com/2011/06/sloped-green-roofs/>> [Accessed 24 Aug. 2021].
- Aqilah, N., Zaki, S.A., Hagishima, A., Rijal, H.B. and Yakub, F., 2021. Analysis on electricity use and indoor thermal environment for typical air-conditioning residential buildings in Malaysia. *Urban Climate*, 37.
- Azis, S.S.A., 2021. Improving present-day energy savings among green building sector in Malaysia using benefit transfer approach: Cooling and lighting loads. *Renewable and Sustainable Energy Reviews*, 137.
- Bergman, T.L., Lavine, A.S., Incropera, F.P. and DeWitt, D.P., 2011. *Fundamentals of heat and mass transfer*. 7th ed. ed. Hoboken, NJ : John Wiley & Sons.
- Bevilacqua, P., 2021. The effectiveness of green roofs in reducing building energy consumptions across different climates. A summary of literature results. *Renewable and Sustainable Energy Reviews*, 151, p.111523.

Bindiganavile, V. and Hoseini, M., 2019. Foamed concrete. In: *Developments in the Formulation and Reinforcement of Concrete*. Woodhead Publishing. pp.365–390.

BMI, 2021. *BMI CoolRoof: Roof cooling system & heat-proof solution*. [online] Available at: <<https://www.bmigroup.com/my/products/roofing-systems/coolroof>> [Accessed 24 Aug. 2021].

Chow, M.F. and Bakar, M.F.A., 2016. A Review on the development and challenges of green roof systems in Malaysia. [online] Available at: <<https://zenodo.org/record/1338620>> [Accessed 24 Aug. 2021].

Claisse, P.A., 2016. Admixtures for concrete. In: *Civil Engineering Materials*. Butterworth-Heinemann. pp.251–258.

Dong, Y., McCartney, J.S. and Lu, N., 2015. Critical review of thermal conductivity models for unsaturated soils. *Geotechnical and Geological Engineering*, 33(2), pp.207–221.

FLL, 2002. *Guidelines for the Planning , Execution and Upkeep of Green-roof sites*. [online] Available at: <[http://www.greenroofsouth.co.uk/FLL Guidelines.pdf](http://www.greenroofsouth.co.uk/FLL_Guidelines.pdf)> [Accessed 6 Apr. 2022].

Hirunlabh, J., Wachirapuwadon, S., Pratinthong, N. and Khedari, J., 2001. New configurations of a roof solar collector maximizing natural ventilation. *Building and Environment*, 36(3), pp.383–391.

Hisham, N.A., Zaki, S.A., Hagishima, A., Yusoff, N.M. and Yakub, F., 2019. Load and household profiles analysis for air-conditioning and total electricity in Malaysia. *KnE Social Sciences*.

Hu, S., Yan, D. and Qian, M., 2019. Using bottom-up model to analyze cooling energy consumption in China's urban residential building. *Energy and Buildings*, 202.

Hui, C.M.S. and Chan, H.-M., 2008. Development of modular green roofs for high-density urban cities. In: *World Green Roof Congress*. [online] Available at: <https://www.researchgate.net/publication/254954155_Development_of_modular_green_roofs_for_high-density_urban_cities> [Accessed 24 Aug. 2021].

Hui, S.C.M., 2011. *Technical guidelines for green roof systems in Hong Kong. Joint Symposium 2010 on Low Carbon High Performance Buildings*, CIBSE Hong Kong Branch.

Ismail, A., Samad, M.H.A. and Rahman, A.M.A., 2008. Using green roof concept as a passive design technology to minimise the impact of global warming. In: *2nd International Conference On Built Environment In Developing Countries (ICBEDC 2008)*. [online] pp.588–598. Available at: <http://eprints.usm.my/25136/1/BUILDING_ENGINEERING_AND_CONSTRUCTION_7.pdf> [Accessed 24 Aug. 2021].

Ismail, Z., Aziz, H.A., Nasir, N.M. and Taib, M.Z.M., 2012. Obstacles to adopt green roof in Malaysia. In: *CHUSER 2012 - 2012 IEEE Colloquium on Humanities, Science and Engineering Research*. [online] pp.357–361. Available at: <<https://ieeexplore.ieee.org/document/6504339>> [Accessed 24 Aug. 2021].

Iyer, N.R., 2020. An overview of cementitious construction materials. *New Materials in Civil Engineering*, pp.1–64.

Khedari, J., Hirunlabh, J. and Bunnag, T., 1996. Experimental study of a Roof Solar Collector towards the natural ventilation of new habitations. *Renewable Energy*, 8(1–4), pp.335–338.

Khedari, J., Ingkawanich, S., Waewsak, J. and Hirunlabh, J., 2002. A PV system enhanced the performance of roof solar collector. *Building and Environment*, 37(12), pp.1317–1320.

Kozłowski, M. and Kadela, M., 2018. Mechanical characterization of

lightweight foamed concrete. *Advances in Materials Science and Engineering*, pp.1–8.

Krishman, R., Ahmad, H. and Mohamad, S., 2013. Malaysia's native plant drought tolerance performance on extensive green roof. In: *4th International Graduate Conference on Engineering, science and Humanities IGCESH*. [online] pp.803–808. Available at: <https://www.academia.edu/3212078/Malaysia_s_Native_Plants_Drought_Tolerance_Performance_On_Extensive_Green_Roof> [Accessed 24 Aug. 2021].

Lee, S., Park, S.H., Yeo, M.S. and Kim, K.W., 2009. An experimental study on airflow in the cavity of a ventilated roof. *Building and Environment*, 44(7), pp.1431–1439.

Malaysian Standard 1525, 2014. *Energy efficiency and use of renewable energy for non-residential buildings - Code of practice*. Second Rev ed. *STANDARDS MALAYSIA 2014 - All rights reserved*. DEPARTMENT OF STANDARDS MALAYSIA.

Ministry of Economic Affairs, 2018. *Mid-Term review of the Eleventh Malaysia Plan, 2016-2020: New priorities and emphases*. [online] *Ministry of Economic Affairs Affairs, Ministry of Economic*. Available at: <[http://www.epu.gov.my/sites/default/files/2020-08/Mid-Term Review of 11th Malaysia Plan.pdf](http://www.epu.gov.my/sites/default/files/2020-08/Mid-Term%20Review%20of%2011th%20Malaysia%20Plan.pdf)>.

Ministry of Energy, 2017. *Green technology master plan Malaysia 2017 - 2030*. [online] Green Technology and Water (KeTTHA). Available at: <<https://www.pmo.gov.my/wp-content/uploads/2019/07/Green-Technology-Master-Plan-Malaysia-2017-2030.pdf>> [Accessed 24 Aug. 2021].

Mohd Sari, K.A. and Mohammed Sani, A.R., 2017. Applications of Foamed Lightweight Concrete. In: *MATEC Web of Conferences*. [online] EDP Sciences. Available at: <https://www.matec-conferences.org/articles/mateconf/pdf/2017/11/mateconf_eti2017_01097.p

df> [Accessed 24 Aug. 2021].

Ng, W.T., Zaki, S.A., Hagishima, A., Rijal, H.B., Zakaria, M.A. and Yakub, F., 2019. Effectiveness of free running passive cooling strategies for indoor thermal environments: Example from a two-storey corner terrace house in Malaysia. *Building and Environment*, 160.

Palmer, B., 2020. *Curing Concrete - How Long it Takes & How To Cure - The Concrete Network*. [online] Available at: <<https://www.concretenetwork.com/curing-concrete/>> [Accessed 24 Aug. 2021].

Pandey, S., Hindoliya, D.A. and Mod, R., 2013. Experimental investigation on green roofs over buildings. *International Journal of Low-Carbon Technologies*, 8(1), pp.37–42.

Ramamurthy, K., Nambiar, E.K.K. and Ranjani, G.I.S., 2009. A classification of studies on properties of foam concrete. *Cement and Concrete Composites*, 31(6), pp.388–396.

Ramlee, N.A., Naveen, J. and Jawaid, M., 2021. Potential of oil palm empty fruit bunch (OPEFB) and sugarcane bagasse fibers for thermal insulation application – A review. *Construction and Building Materials*, 271.

Ranjbar, N., Zaki, S.A., Yusoff, N.M. and Hagishima, A., 2017. Time series data analysis of household electricity usage during El-Nino in Malaysia. *Chemical Engineering Transactions*, 56, pp.379–384.

Ravindra, K.D. and Michael, J.M., 1996. *Appropriate Concrete Technology*. *Appropriate Concrete Technology*. E & FN SPON.

Sena, B., Zaki, S.A., Rijal, H.B., Ardila-Rey, J.A., Yusoff, N.M., Yakub, F., Ridwan, M.K. and Muhammad-Sukki, F., 2021. Determinant factors of electricity consumption for a Malaysian household based on a field survey.

Sustainability (Switzerland), 13(2), pp.1–31.

Shaikh, P.H., Nor, N.B.M., Sahito, A.A., Nallagownden, P., Elamvazuthi, I. and Shaikh, M.S., 2017. Building energy for sustainable development in Malaysia: A review. *Renewable and Sustainable Energy Reviews*, 75, pp.1392–1403.

Siew, Z.B., Chin, C.M. and Sakundarini, N., 2019. Designing a guideline for green roof system in Malaysia. *Journal Clean WAS (JCleanWAS)*, 3(2), pp.5–10.

Suruhanjaya Tenaga, 2017a. *Energy statistic Malaysia handbook*. [online] SURUHANJAYA TENAGA (ENERGY COMMISSION). Available at: <https://www.st.gov.my/contents/files/download/116/Malaysia_Energy_Statistics_Handbook_2017.pdf> [Accessed 24 Aug. 2021].

Suruhanjaya Tenaga, 2017b. *National energy balance*. [online] SURUHANJAYA TENAGA (ENERGY COMMISSION). Available at: <<https://meih.st.gov.my/documents/10620/f85ba3ae-fd44-4ea4-a69d-400c5f96b3ea>> [Accessed 24 Aug. 2021].

Suruhanjaya Tenaga, 2019. *Malaysia energy statistic handbook*. [online] SURUHANJAYA TENAGA (ENERGY COMMISSION). Available at: <<https://meih.st.gov.my/documents/10620/bcce78a2-5d54-49ae-b0dc-549dcacf93ae>> [Accessed 24 Aug. 2021].

Tan, P.Y. and Sia, A., 2008. *A selection of plants for green roofs in Singapore*. 2nd Editio ed. *National park Board*, Singapore: Centre for Urban Greenery and Ecology.

Tang, C. and Chin, N., 2017a. *Building energy efficiency technical guideline for active design*. [online] Building Sector Energy Efficiency Project (BSEEP).

Tang, C. and Chin, N., 2017b. *Building energy efficiency technical guideline for passive design*. Building Sector Energy Efficiency Project (BSEEP).

Tho, V.D., Korol, E. and Hoang, N.H., 2018. Analysis of the effectiveness of thermal insulation of a multi-layer reinforced concrete slab using layer of concrete with low thermal conductivity under the climatic conditions of Vietnam. In: *MATEC Web of Conferences*. [online] EDP Sciences. Available at: <<https://doi.org/10.1051/mateconf/201825104026>> [Accessed 24 Aug. 2021].

U.S. Department of Energy, 2016. *Annual energy outlook 2016 with projections to 2040*. [online] Available at: <<https://www.osti.gov/biblio/1329373>>.

Yew, M.C., Ramli Sulong, N.H., Chong, W.T., Poh, S.C., Ang, B.C. and Tan, K.H., 2013. Integration of thermal insulation coating and moving-air-cavity in a cool roof system for attic temperature reduction. *Energy Conversion and Management*, 75, pp.241–248.

Yew, M.C., Yew, M.K., Ho, M.L. and Saw, L.H., 2021. Integration of lightweight foam concrete Roof, moving-air-cavity, and solar-powered fans for attic temperature reduction. *Frontiers in Built Environment*, p.7.

Yew, M.C., Yew, M.K., Saw, L.H. and Durairaj, R., 2017. Integration of active and passive cool roof system for attic temperature reduction. In: *AIP Conference Proceedings*. [online] AIP Publishing LLC AIP Publishing.p.020023. Available at: <<https://aip.scitation.org/doi/abs/10.1063/1.4979394>> [Accessed 24 Aug. 2021].

Yew, M.C., Yew, M.K., Saw, L.H., Ng, T.C., Chen, K.P., Rajkumar, D. and Beh, J.H., 2018. Experimental analysis on the active and passive cool roof systems for industrial buildings in Malaysia. *Journal of Building Engineering*, 19, pp.134–141.

Zhao, S.B., Yang, S., Feng, X.Z. and Lu, M.J., 2013. Study on thermal conductivity of reinforced concrete plate. *Applied Mechanics and Materials*, 438–439, pp.321–328.

ZinCo, n.d. *Systems for Pitched Green Roofs More Options with ZinCo*. [online]

ZinCo GmbH. Available at: <www.zinco-greenroof.com> [Accessed 24 Aug. 2021].

APPENDICES

Appendix A: Figures



Figure A-1: Backbone of the MAC.



Figure A-2: Roof Model I (Reinforced Concrete Roof Slab).



Figure A-3: Roof Model II (LFC Roof Slab).



Figure A-4: Roof Model III (LFC Roof Slab with MAC).



Figure A-5: Roof Model IV (LFC Roof Slab with Active MAC Fitted with S-P Fs).

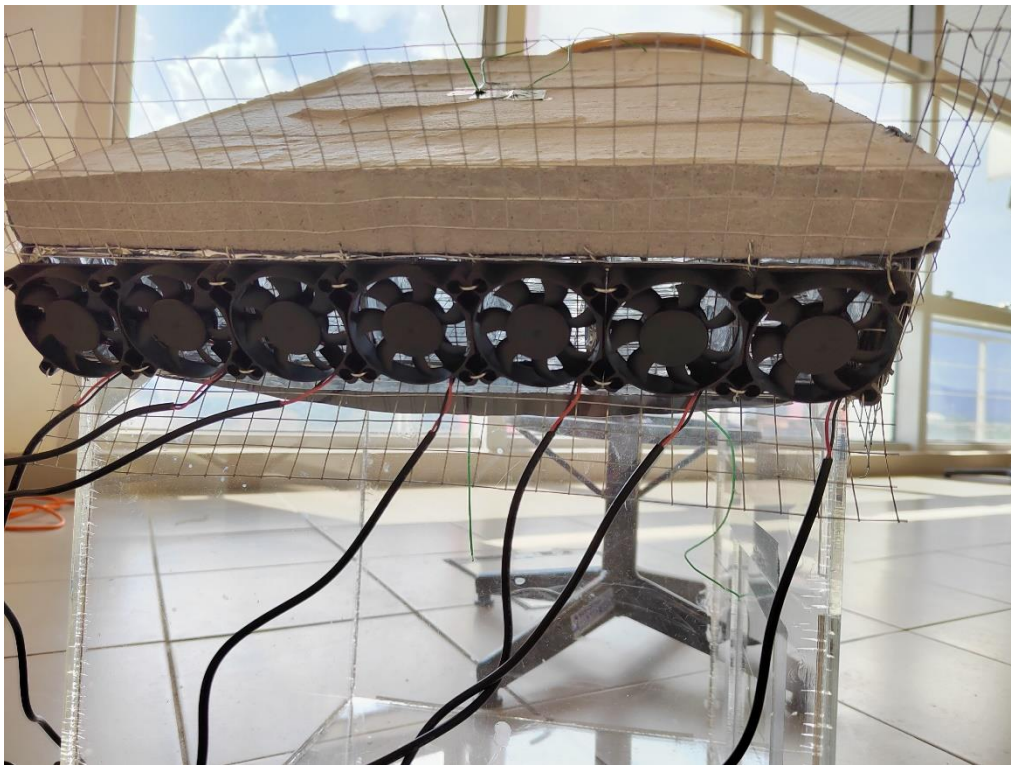


Figure A-6: S-P Fs Installed at the Inlet of the MAC.



Figure A-7: Roof Model V (LFC Roof Slab Topped with Vegetation Layer with Active MAC Fitted with S-P Fs).

Appendix B: Tables

Table B- 1: Results for Roof Model I (Reinforced Concrete Roof Slab).

Time (min)	Temperature (°C)		
	Roof Surface (T1)	Attic (T2)	Ambient (T3)
0	27.8	27.5	27.0
1	28.1	27.6	31.0
2	28.5	27.7	30.6
3	28.8	27.8	31.0
4	29.1	28.0	31.4
5	29.4	28.1	31.5
6	30.0	28.3	32.0
7	30.2	28.4	31.5
8	30.4	28.5	31.7
9	30.9	28.6	32.6
10	31.2	28.7	31.7
11	31.5	28.8	32.0
12	31.8	28.9	32.4
13	32.1	29.0	32.4
14	32.4	29.1	32.9
15	32.8	29.2	33.0
16	33.3	29.3	32.4
17	33.4	29.4	32.4
18	33.9	29.4	31.8
19	34.2	29.5	31.3
20	34.5	29.6	32.6
21	34.7	29.6	32.2
22	35.2	29.7	32.3
23	35.4	29.8	32.7
24	35.6	29.8	32.3
25	36.0	29.9	31.8
26	36.3	30.0	31.3
27	36.5	30.1	31.7
28	36.9	30.2	31.3
29	37.2	30.3	31.7
30	37.5	30.3	32.2

Table B-2: Results for Roof Model II (LFC Roof Slab).

Time (min)	Temperature (°C)		
	Roof Surface (T1)	Attic (T2)	Ambient (T3)
0	27.3	27.5	27.1
1	28.5	27.5	30.5
2	29.2	27.7	30.2
3	29.7	27.7	31.0
4	30.4	27.8	31.4
5	30.9	28.1	31.1
6	31.3	28.1	30.9
7	31.9	28.2	30.7
8	32.3	28.3	31.4
9	33.1	28.5	32.1
10	33.4	28.7	31.1
11	33.9	28.7	32.6
12	34.2	28.7	32.2
13	34.8	28.8	31.8
14	35.1	29.0	31.6
15	35.8	29.1	32.0
16	36.3	29.2	31.5
17	36.7	29.3	32.2
18	37.0	29.3	32.0
19	37.7	29.4	32.1
20	38.2	29.5	32.0
21	38.0	29.5	32.1
22	38.4	29.6	32.1
23	38.7	29.7	33.6
24	39.2	29.8	32.8
25	39.3	29.9	32.5
26	40.2	30.0	32.5
27	40.8	30.0	32.3
28	40.5	30.1	32.5
29	40.4	30.2	32.5
30	40.4	30.2	32.5

Table B-3: Results for Roof Model III (LFC Roof Slab with MAC).

Time (min)	Temperature (°C)			
	Roof Surface (T1)	Attic (T2)	Ambient (T3)	MAC (T4)
0	27.3	27.4	27.3	27.3
1	29.4	27.5	32.8	27.5
2	30.5	27.5	34.3	27.5
3	31.5	27.5	34.1	27.5
4	32.5	27.6	33.9	27.6
5	33.1	27.6	34.5	27.8
6	34.0	27.7	34.2	27.9
7	34.8	27.8	35.2	28.0
8	35.7	27.9	35.6	28.1
9	36.6	27.9	35.7	28.3
10	36.9	28.1	35.7	28.4
11	37.4	28.1	35.0	28.8
12	38.4	28.2	34.5	28.8
13	38.9	28.3	34.3	29.3
14	39.4	28.3	34.1	29.1
15	40.4	28.4	34.9	29.1
16	41.0	28.4	35.1	29.2
17	41.5	28.5	34.7	29.1
18	42.1	28.5	33.8	29.6
19	42.6	28.6	34.8	29.3
20	43.2	28.6	34.7	29.7
21	43.3	28.7	35.4	30.3
22	44.2	28.7	35.3	30.3
23	44.6	28.7	34.6	30.2
24	44.9	28.8	34.7	30.4
25	45.7	28.8	34.5	30.1
26	45.7	28.8	34.0	30.3
27	47.0	28.9	34.9	29.8
28	47.2	28.9	35.0	30.2
29	48.0	28.9	36.1	29.6
30	47.8	28.9	35.8	29.7

Table B-4: Results for Roof Model IV (LFC Roof Slab with Active MAC Fitted with S-P Fs).

Time (min)	Temperature (°C)			
	Roof Surface (T1)	Attic (T2)	Ambient (T3)	MAC (T4)
0	27.6	27.3	27.0	27.4
1	29.4	27.3	29.9	27.6
2	30.4	27.4	30.9	27.8
3	31.6	27.4	30.5	28.1
4	32.1	27.5	30.2	28.1
5	32.7	27.5	30.7	28.3
6	33.3	27.5	31.2	28.2
7	34.2	27.5	30.6	28.3
8	34.7	27.6	31.2	28.5
9	35.3	27.6	30.7	28.5
10	35.8	27.6	30.5	28.5
11	36.5	27.7	31.2	28.6
12	37.4	27.6	31.0	28.7
13	37.7	27.7	30.9	29.0
14	38.0	27.8	31.1	28.8
15	39.0	27.8	31.2	28.8
16	39.3	27.8	31.6	29.2
17	39.8	27.9	31.2	29.2
18	40.7	27.9	32.0	29.5
19	41.1	27.9	31.5	29.5
20	41.8	27.9	31.3	29.4
21	42.0	28.0	31.7	29.4
22	42.9	28.0	31.1	29.4
23	43.0	28.0	31.7	29.4
24	43.4	28.1	32.5	29.5
25	44.1	28.1	32.5	29.9
26	44.4	28.1	32.3	29.7
27	44.9	28.1	31.3	29.7
28	45.3	28.2	31.4	29.9
29	45.5	28.2	31.9	29.9
30	45.6	28.2	31.3	29.9

Table B-5: Results for Roof Model V (LFC Roof Slab Topped with Vegetation Layer with Active MAC Fitted with S-P Fs).

Time (min)	Temperature (°C)				
	Roof Surface (T1)	Attic (T2)	Ambient (T3)	MAC (T4)	Soil (T5)
0	26.7	26.8	25.7	25.7	23.8
1	26.6	26.8	28.2	26.0	24.3
2	26.5	26.9	29.2	26.3	24.8
3	26.6	26.9	28.5	26.2	25.2
4	26.5	26.8	30.1	26.4	25.5
5	26.5	26.8	30.3	26.5	25.8
6	26.5	26.9	29.8	26.4	26.1
7	26.5	26.9	29.4	26.4	26.3
8	26.4	26.9	29.4	26.5	26.5
9	26.4	26.9	29.1	26.5	26.8
10	26.4	26.9	29.6	26.5	27.0
11	26.4	26.9	29.2	26.5	27.3
12	26.3	26.9	32.7	26.6	27.6
13	26.3	26.9	30.9	26.5	27.7
14	26.3	26.9	33.7	26.6	27.9
15	26.3	26.9	30.8	26.5	28.0
16	26.3	26.9	30.6	26.6	28.1
17	26.2	26.9	32.8	26.6	28.3
18	26.2	26.9	32.7	26.7	28.5
19	26.2	26.9	31.3	26.6	28.6
20	26.2	26.9	30.7	26.7	28.7
21	26.1	26.9	32.7	26.8	28.9
22	26.1	26.9	30.2	26.8	29.0
23	26.1	26.9	30.1	26.7	29.4
24	26.1	26.9	30.0	26.8	29.7
25	26.0	26.9	30.8	26.9	29.9
26	26.0	26.9	30.4	26.8	29.9
27	26.0	26.9	30.4	26.8	30.1
28	26.0	26.9	30.3	26.8	30.3
29	26.0	26.9	30.9	26.9	30.4
30	26.0	26.9	30.5	26.8	30.5